

24/06/2016

Master Thesis

Fabrication of bulk
nanostructured magnetic
materials based on Sm-Fe-N
alloy doped with zinc

Author:
Johan LOISON

Supervisor:
Dr. Vladimir An, TPU

*A thesis submitted in fulfilment of the
requirements for the degree of Master of Science
in the
Department of Nanomaterials and
Nanotechnology, TPU
PhITEM UJF*

Министерство образования и науки Российской Федерации
Федеральное государственное автономное образовательное
учреждение высшего образования
«НАЦИОНАЛЬНЫЙ ИССЛЕДОВАТЕЛЬСКИЙ ТОМСКИЙ
ПОЛИТЕХНИЧЕСКИЙ УНИВЕРСИТЕТ»

Институт физики высоких технологий

Направление подготовки 22.04.01 «Материаловедение и технологии материалов»

Кафедра наноматериалов и нанотехнологий

МАГИСТЕРСКАЯ ДИССЕРТАЦИЯ

**Fabrication of bulk nanostructured magnetic materials based on
Sm-Fe-N alloy doped with Zn**

Студент

Группа	ФИО	Подпись	Дата
4БМ4И1	ЛУАЗОН ЖОАН ПЬЕР		

Руководитель

Должность	ФИО	Ученая степень, звание	Подпись	Дата
доцент	АН В. В.	К.т.н.		

КОНСУЛЬТАНТЫ:

По разделу «Финансовый менеджмент, ресурсоэффективность и ресурсосбережение»

Должность	ФИО	Ученая степень, звание	Подпись	Дата
доцент	Лямина Г.В.	К.х.н.		

По разделу «Социальная ответственность»

Должность	ФИО	Ученая степень, звание	Подпись	Дата
доцент	Лямина Г.В.	К.х.н.		

ДОПУСТИТЬ К ЗАЩИТЕ:

профессор	ФИО	Ученая степень, звание	Подпись	Дата
Наноматериалов и нанотехнологий	Олег Леонидович Хасанов	Д.т.н., проф.		

Планируемые результаты обучения
по ООП 22.04.01 «Материаловедение и технологии материалов»,
профиль «Производство изделий из наноструктурных материалов»

Код результата	Результат обучения
Р1	Осуществлять сбор, анализ и обобщение научно-технической информации в области материаловедения и технологии материалов с использованием современных информационно-коммуникационных технологий, глобальных информационных ресурсов
Р2	Работать с патентным законодательством и авторским правом при подготовке документов к патентованию и оформлению ноу-хау
Р3	Выполнять маркетинговые исследования и анализировать технологический процесс как объекта управления, разрабатывать технико-экономическое обоснование инновационных решений в профессиональной деятельности
Р4	Руководить коллективом в сфере своей профессиональной деятельности, толерантно воспринимая социальные, этнические, конфессиональные и культурные различия
Р5	Внедрять в производство технологии получения керамических, металлических материалов и изделий, в том числе наноматериалов, быть готовым к профессиональной эксплуатации современного оборудования и приборов, позволяющих получать и диагностировать материалы и изделия различного назначения.
Р6	Разрабатывать новые и модернизировать существующие технологии получения керамических, металлических материалов и изделий, в том числе наноматериалов
Р7	Внедрять системы управления качеством продукции в области материаловедения, эксплуатировать оборудование, позволяющее диагностировать материалы и изделия из них, в том числе наноматериалы
Р8	Действовать в нестандартных ситуациях, нести социальную и этическую ответственность за принятые решения, выбирать наиболее рациональные способы защиты и порядка в действиях малого коллектива в чрезвычайных ситуациях
Р9	Общаться в устной и письменной формах на иностранном языке для решения задач профессиональной деятельности, подготавливать и представлять презентации планов и результатов собственной и командной деятельности, формировать и отстаивать собственные суждения и научные позиции
Р10	Самостоятельно осваивать новые методы исследования, изменять научный, научно-педагогический и производственный профиль своей профессиональной деятельности
Р11	Применять принципы рационального использования природных ресурсов, основные положения и методы социальные, гуманитарные и экономические подходы при решении профессиональных задач с учётом последствий для общества, экономики и экологии.
Р12	Использовать основные категории и понятия общего и производственного менеджмента в профессиональной деятельности

Министерство образования и науки Российской Федерации
федеральное государственное автономное образовательное учреждение
высшего образования
**«НАЦИОНАЛЬНЫЙ ИССЛЕДОВАТЕЛЬСКИЙ
ТОМСКИЙ ПОЛИТЕХНИЧЕСКИЙ УНИВЕРСИТЕТ»**

Институт физики высоких технологий

Направление подготовки 22.04.01 «Материаловедение и технологии материалов»

Кафедра наноматериалов и нанотехнологий

УТВЕРЖДАЮ:

Зав. кафедрой

О.Л. Хасанов

(подпись)

(дата)

ЗАДАНИЕ
на выполнение выпускной квалификационной работы

В форме:

магистерской диссертации

Студенту:

Группа	ФИО
4БМ4И1	ЛУАЗОН ЖОАН ПЬЕР

Тема работы:

Получение объемных наноструктурных магнитных материалов на основе сплава Sm-Fe-N, допированного цинком

Утверждена приказом директора

№2599 от 06/04/2016

Срок сдачи студентом выполненной работы:

ТЕХНИЧЕСКОЕ ЗАДАНИЕ:

Исходные данные к работе	Цель работы – Study of the microstructure of Zinc doped, Sm-Fe-N ceramics produced by Spark Plasma Sintering (SPS) to improve its mechanical and magnetic properties. Исследуемые материалы: Sm-Fe-N powder, Zinc powder, based on Sm-Fe-N magnetic ceramics
---------------------------------	---

<p>Перечень подлежащих исследованию, проектированию и разработке вопросов</p>	<p>Tasks</p> <ol style="list-style-type: none"> 1. Description of mechanical and magnetic properties of initial powders (SmFeN, Zn) 2. State of the art 3. Description and choice of the experimental techniques 4. Description of mechanical and magnetic properties of SMFEN bases ceramics 5. Reflexion on the analysis results 6. Financial management 7. Social responsibility
--	--

Консультанты по разделам выпускной квалификационной работы

(с указанием разделов)

Раздел	Консультант
1. Обзор литературы 2. Объект и методы исследования 3. Результаты проведенного исследования	Ан Владимир Вилорьевич
Финансовый менеджмент, ресурсоэффективность и ресурсосбережение	<i>Галина Владимировна Лямина</i>
Социальная ответственность	<i>Галина Владимировна Лямина</i>
Иностранный язык	

Названия разделов, которые должны быть написаны на русском и иностранном языках:

Разделы на английском языке: введение, литературный обзор, оборудование и методики исследования, экспериментальная часть, заключение, финансовый менеджмент, ресурсоэффективность и ресурсосбережение; социальная ответственность

Дата выдачи задания на выполнение выпускной квалификационной работы по линейному графику

Задание выдал руководитель:

Должность	ФИО	Ученая степень, звание	Подпись	Дата
доцент	В. В. АН	К.т.н.		

Задание принял к исполнению студент:

Группа	ФИО	Подпись	Дата
4БМ4И1	ЛУАЗОН ЖОАН ПЬЕР		

Definitions, designations, acronyms, normative

references

Sm-Fe-N: Samarium Iron Nitride

Zn: Zinc

SPS: Spark Plasma Sintering

XRD: X-Ray Diffraction

SEM: Scanning Electron Microscope

Magnetic materials: Materials having a specific behaviour under magnetic field

Paramagnetic materials: Magnetic materials presenting a magnetisation when disposed under magnetic field

Ferromagnets: Paramagnetic materials with coupling of spins in the same direction

B_r = Magnetization of remanence

B_s = Magnetization of saturation

H_C = Field of coercivity

Tomsk Polytechnic University

Joseph Fourier University

Abstract

Master of Science

Fabrication of bulk nanostructured magnetic materials based on
Sm-Fe-N alloy doped with zinc

By Johan Pierre LOISON

Neodymium based permanent magnets need during their elaboration an addition of Dysprosium. Dy is an expensive rare earth element, which increases the price of industrialisation. To replace Nd-Fe-B permanent magnets Sm-Fe-N alloy is nowadays one of the best candidate. Indeed its magnetic properties (remanence and coercivity), and its Curie temperature are suitable for high temperature magnetic applications ($M_r=1,26T$, $H_c = 1114$ kA/m, $T_c=749$). However, because of its decomposition on the soft and hard magnetic phases at temperature higher than 500°C , the main challenge is the elaboration of fabrication technique for mass production. The way to obtain highly dense magnetic ceramics is to use unconventional compaction techniques (with high pressure, or/and special sintering machines) and sometimes the use of metallic or polymer binders. In this work the fabrication of magnetic ceramics with an addition of Zinc by spark plasma sintering technique is discussed. The analysis of its microstructure and magnetic properties is presented. Based on the analysis of experimental results the way to produce highly dense magnetic ceramics with improved magnetic properties is found.

Content

Definitions, designations, acronyms, normative references	5
Abstract	6
Content	7
List of Figures	8
List of tables:	9
Introduction:	10
I. Chapter 1: Review on advanced magnetic materials	11
A. Magnetic properties	11
1. Definition of magnetic materials	11
2. Ferromagnets	14
3. Property and definition of coercivity	17
B. Magnetic materials for permanent magnets	22
II. Chapter 2: Elaboration and characterisation of Sm-Fe-N permanent magnet... ..	26
A. State of the art	26
1. Sintering of $\text{Sm}_2\text{Fe}_{17}\text{N}_3$ by non-conventional techniques	26
2. Use of binders	28
B. Description of the techniques	30
1. The Spark Plasma Sintering (SPS) technique	30
2. X-Ray Diffraction (XRD) analysis	33
3. Scanning Electron microscopy (SEM)	35
4. Extraction magnetometry	38
III. Chapter 3: Experimental procedure	42
A. Powder preparation	42
B. Magnetic pre-alignment	45
C. SPS procedure	46
D. Analysis	47
IV. Chapter 5: Financial management	49
Raw materials, purchased products	49
V. Chapter 6: Social impact	Erreur ! Signet non défini.
Potential consumers of research results	Erreur ! Signet non défini.
VI. References	Erreur ! Signet non défini.

List of Figures

Figure I-1: Periodic table of elements, showing which elements present magnetic properties. In red, the element where magnetic order can be found in solid state. In orange is antiferromagnetic elements. In green is ferromagnetic elements.	11
Figure I-2: Periodic table of elements, showing which elements present magnetic properties. In red, the element where magnetic order can be found in solid state. In orange is antiferromagnetic elements. In green is ferromagnetic elements.	11
Figure I-3: Representation of ferromagnetic coupling (a) and anti-ferromagnetic coupling (b)	12
Figure I-4: Magnetic behaviour of ferromagnetic, paramagnetic, and diamagnetic materials under a magnetic field H.	12
Figure I-5: Effect of temperature on magnetic moment of ferromagnets.....	13
Figure I-6: Representation of the Weiss domains, Bloch walls, and their behaviours while exposed to a growing magnetic field. (From the left to the right).....	14
Figure I-7: Typical hysteresis loop for permanent magnet, showing the position of the different value we can extract from it. Coercivity, Remanence, and Saturation.....	15
Figure I-8: B(BH) plot, used to find $(BH)_{max}$	15
Figure I-9: Draw of a particle under a magnetic field H, the magnetization M, and the easy axis in dashed line	18
Figure I-10: Schematic of the energy barrier in the case of a uni-axial system with no external applied magnetic field.	18
Figure I-11: Evolution of the energy barrier in the presence of an increasing magnetic field.	19
Figure I-12: Schematic representing coherent rotation in uni-axial systems.....	20
Figure I-13: Depiction of magnetization reversal in the case of nucleation pinning reversal mechanism.	21
Figure I-14: Evolution of the energy product $(BH)_{max}$ with the development of magnetic materials	22
Figure I-15: Classification of magnets depending of the temperature dependence.....	25
Figure II-1 Coercivity observed for different grain size. Top for sintered and down for powder. E-1 μ m D-2 μ m C-5 μ m (12)	26
Figure II-2-1: Low-magnification SEM BSE images of (a) as-sintered (low coercivity) and (b) post-sinter-annealed (high coercivity) samples (coercivity values are shown in the inset). Relatively high-magnification images of the post-sinter-annealed sample showing the formation of (c) particle boundary and (d) grain boundary phase. (9).....	29
Figure II-3: Representation of the grain growth and the formation of the grain boundary in the four stages. Loose, initial, intermediate and final stages.....	31
Figure II-4: Schema of the SPS device, including, the press, the controller, and generator.....	32
Figure II-5: Temperature gradients in macroscopic view, and local view. In local view we can see the increase of the temperature on the part of the neck.	32
Figure II-6: General scheme of a X-Ray diffractometer.	34
Figure II-7: Scheme of the composition and the functioning of a Scanning Electron Microscope	35
Figure II-8: Representation of the interaction of electrons with the surface, and the interaction observed with a SEM.	36
Figure II-9: Different type of magnetometer, (commercial, and laboratory) and their different capacities.	39
Figure II-10: Graph showing the principle of measure of an extraction magnetometer	40
Figure II-11: Scheme of an extraction magnetometer.....	41
Figure III-1: SEM picture of $Sm_2Fe_{17}N_3$ to give an idea of the size repartition	42
Figure III-2: SEM picture of the Zn powder	43
Figure III-3: XRD analysis of 15%Zn+ $Sm_2Fe_{17}N_3$ powder. In red $Sm_2Fe_{17}N_3$, in blue Zn, in green α Fe.	44
Figure III-4: Picture of Zn + $Sm_2Fe_{17}N_3$ mixture in hexane after ultrasonic bath.(left) SEM picture of the mixture (right).	44
Figure III-5: Picture of the device use to pre-align the powder.....	45
Figure III-6: Representation of the effect of magnetic field on the particles during the pre-alignment. On the left, before alignment, the magnetic moments are randomly oriented. On the right, after pre-alignment, the moment of each particle is aligned in the same direction than the magnetic field.....	45
Figure III-7: Compaction curve of the sample 400-8n. In abscise the time is without units. The vertical scale is in cm, it is the displacement of the punch during the compaction.....	47

List of tables:

<i>Table I-1: Approximate values of magnetic susceptibility of different kind of materials</i>	<i>13</i>
<i>Table I-2: Different value of the remanence, coercivity, Curie temperature and theoretical BH product for widely used magnets</i>	<i>16</i>
<i>Table II-1: Densities obtain for different temperatures of sintering under high pressure (13)</i>	<i>27</i>
<i>Table V-1: Raw materials, components and semi-finished products purchased.....</i>	<i>48</i>
<i>Table V-1: Raw materials, components and semi-finished products purchased.....</i>	<i>49</i>
<i>Table V-2: Price of the device and cost of utilisation</i>	<i>50</i>

Introduction:

Magnetic materials have many applications such as information storage or motor realisation. For different applications characteristics of magnets should be different. For vehicle applications (in motors) the material must be a permanent magnet with good magnetic stability in front of the temperature (high Curie temperature), an external magnetic field (high coercivity), and it must also have high magnetisation (see Chapter I Review on advanced magnetic materials). Since the discovery of lanthanides and their properties, it appears to be very efficient to use them in magnetic materials alloys (for their high number of spin) with magnetic metals such as Iron. Nowadays the most known and efficient magnetic alloy is $\text{Nd}_2\text{Fe}_{14}\text{B}$ which is used as permanent magnet in industry (1). This alloy has good physical and magnetic properties, but to obtain these properties in bulk form an addition of Dy and Tb is required. These heavy rear-earth elements are very expensive and their addition creates a huge increase of the price, this is why researchers try to explore other alloys to avoid the use of Dy and Tb. Between these alloys one exhibits even better magnetic properties, it is $\text{Sm}_2\text{Fe}_{17}\text{N}_3$. However, to obtain good magnets we need to obtain a bulk material with high density. For the Sm-Fe-N alloy, this is the major problem, the need to sinter at low temperature to avoid the apparition of soft magnetic phase leads to a low density. This density, does not allow to use it in industry. In this review, we will see different techniques which have been used to improve the densification process and magnetic properties. In the first chapter the definition of magnetism, its origins and main types of magnetic materials will be presented. In the second chapter we will speak about the characteristics of $\text{Sm}_2\text{Fe}_{17}\text{N}_3$ and the previous studies carried out. Then in the third chapter we will see the experimental part, the fabrication technique, and how the analysis has been done. In the fourth chapter the analysis of the results, and the correlation with the expectations will be presented. Then in the fifth chapter we will speak about the economic and social impact. Finally we will end this thesis with the conclusion and the future prospects.

I. Chapter 1: Review on advanced magnetic materials

Some materials, such as the ferrite in the nature, present a magnetic behaviour. In this part we will see what these properties are and where they come from.

A. Magnetic properties

1. Definition of magnetic materials

Magnetism is a class of physical phenomena that are mediated by magnetic fields. A material which present magnetic properties is sensible and has a specific behaviour in front a magnetic field. These materials are called a paramagnetic materials, in opposition with the diamagnetic materials. Having such properties means being able to possess a magnetization of magnetic moment when disposed under magnetic field. Paramagnetic materials contain unpaired electron(s). It's the spin of this (these) electron(s) which will have an orientated precession under the magnetic



Figure I-1: Periodic table of elements, showing which elements present magnetic properties. In red, the element where magnetic order can be found in solid state. In orange is antiferromagnetic elements. In green is ferromagnetic elements.

field (called Larmor precession). The elements presenting magnetic behaviour are shown in figure I-1.

However, there is a group of magnetic materials which do have magnetic moments without an external magnetic field. These materials are called ferromagnetic (cf. figure I-1) (in opposition with anti-ferromagnetic). The character ferro- or anti-ferromagnetic depends of the coupling between the magnetic moments of the atoms of the element. If the moments are all in the same direction after magnetisation, then the material is ferromagnetic and has a magnetic moment. If they are in opposite direction then it is an anti-ferromagnetic material. (cf figure I-2)

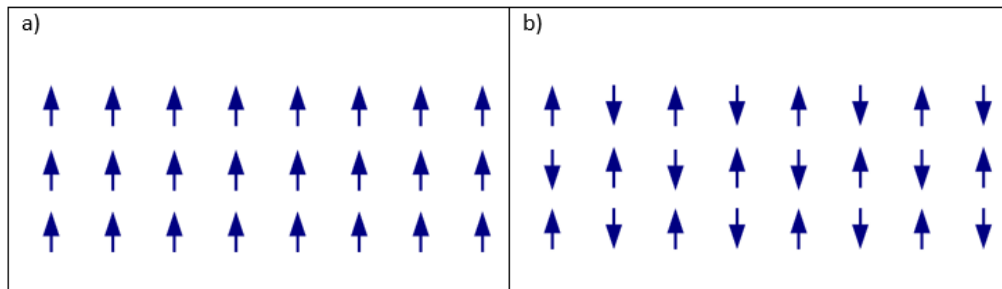


Figure I-3: Representation of ferromagnetic coupling (a) and anti-ferromagnetic coupling (b)

The different behaviour of these materials in front a magnetic field is describe in figure I-3. We can see, that the ferromagnets are then the most sensible materials. The paramagnetic materials behave with a linear magnetization and the diamagnetic with a negative magnetization.

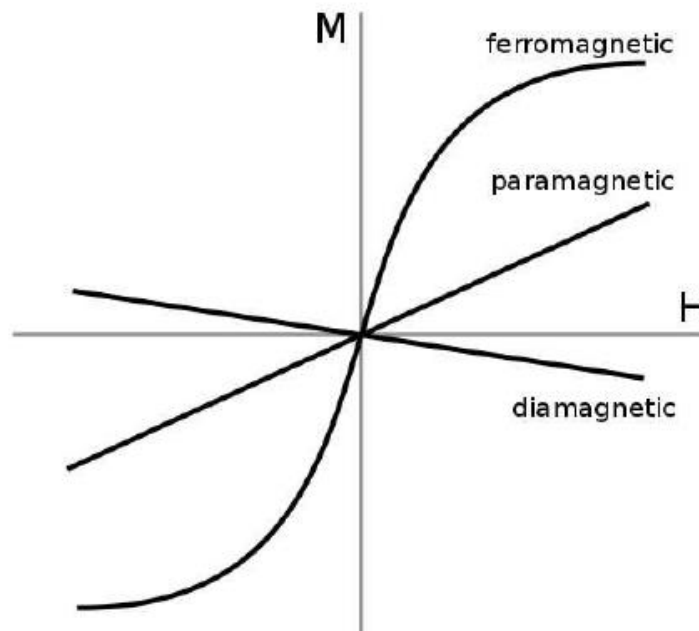


Figure I-4: Magnetic behaviour of ferromagnetic, paramagnetic, and diamagnetic materials under a magnetic field H.

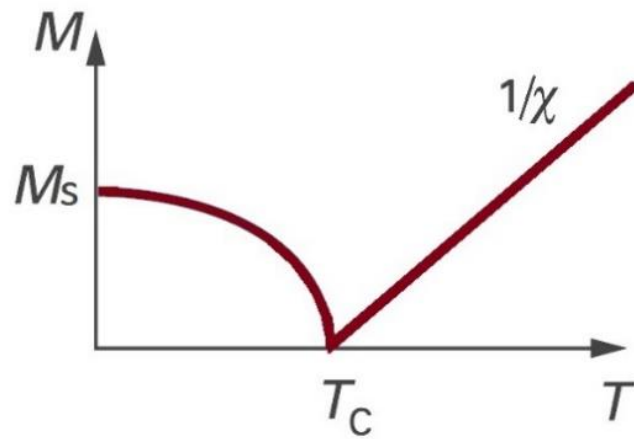


Figure I-5: Effect of temperature on magnetic moment of ferromagnets

A ferromagnetic material has its magnetic moment depending of the temperature (cf. figure 1-4). Indeed, when reach a certain temperature, called Curie Temperature (T_C), then the orientation of the spin is not stable anymore and the material behaves as a paramagnetic material.

In addition, superconductive materials in extremely low temperatures can possess magnetic moment, which specifies its levitation in magnetic field. The application of the external magnetic field induce the magnetic moment in the materials.

The magnetic susceptibility (χ) is a very useful variable to describe the behaviour of magnetic materials.

$$\chi = M/H \quad (1)$$

Where M is the magnetization and H is the magnetic field. For a long period of time magnetic materials were described by this characteristic (Table 1). In general, higher the density of unpaired electrons better is the susceptibility.

Table I-1: Approximate values of magnetic susceptibility of different kind of materials

Material	Magnetic susceptibility
Diamagnetic	$\chi < 0; \chi \approx 10^{-6} \dots 10^{-7}$
Paramagnetic	$\chi > 0; \chi \approx 10^{-4} \dots 10^{-6}$

Antiferromagnetic	$\chi > 0; \chi \approx 10^{-2} \dots 10^{-5}$
Ferro-, ferromagnetic	$\chi \approx 10 \dots 10^6$

2. Ferromagnets

Ferromagnets, as paramagnets, have atomic magnetic moments strongly coupled together. These moments are aligned over regions of the material called Weiss domains. If a ferromagnet has a zero global magnetization it means that the moments in the Weiss domains are randomly aligned without any preferential direction. These domains are affected by defects, inclusions, and dislocations in the material, they have to minimize the energy in the material. The walls between the different domains are called Bloch walls, from Felix Bloch who was the first to study the properties of these zones. They have an associated energy and can respond to an applied field. In a material, an applied field induces a torque on the magnetic moment that forces them to follow the field direction. The Bloch walls move and the Weiss domains parallel to the field start growing (cf. figure 1-5).

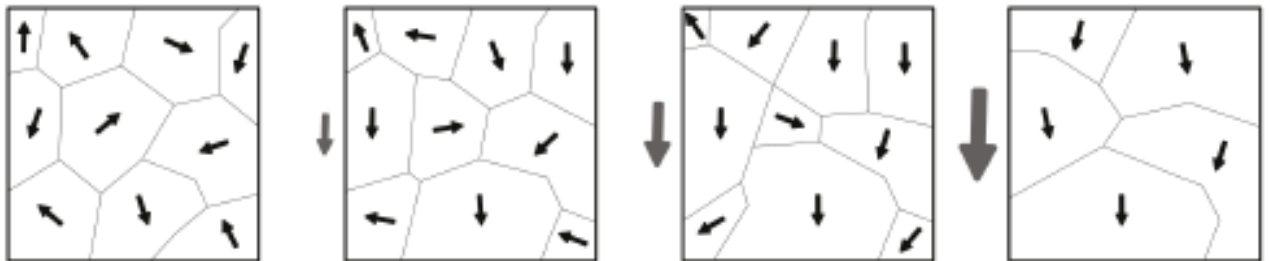


Figure 1-6: Representation of the Weiss domains, Bloch walls, and their behaviours while exposed to a growing magnetic field. (From the left to the right).

This movement of walls in ferromagnets leads to a hysteresis on the loop of magnetisation. To obtain the saturated state, we have to keep a magnetic field H . Because not all the moments reorient when the field is removed, we obtain what is called a remanent magnetisation. For ferromagnetic materials the main characteristics are the remanent magnetization (B_r), the coercivity (H_c), the energy product $(BH)_{\max}$, and the saturation (B_s). They can all be determinate from the magnetic hysteresis loop (figure 1-6).

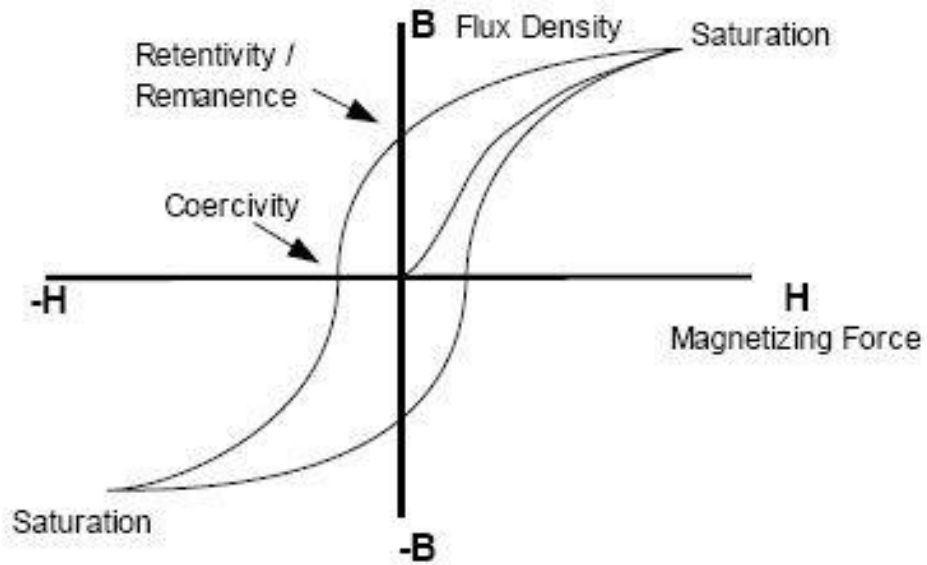


Figure I-7: Typical hysteresis loop for permanent magnet, showing the position of the different value we can extract from it. Coercivity, Remanence, and Saturation.

Hysteresis loop describes the behaviour of ferromagnetic material under applied magnetic field. The curve in the figure I-6 shows the dependence of the magnetic induction B on the external magnetic field H . In the initial state, the sample is fully demagnetized. When the magnetic field H is rising, the induction B will also increase until it reaches the saturation value B_s . When the value of magnetic field drops to zero, the ferromagnetic material still have a remanent magnetization B_r . If an external magnetic field of a reversed sign is applied to the sample, it will cause the demagnetization of the material and the induction B becomes zero at a certain value of applied field. This value called coercive field H_c . It simply describes the value of the field which is needed to fully demagnetize the material. Every point on the curve corresponds to a certain value of magnetic induction B and magnetic field H . The energy product is calculated during the demagnetisation curve. It is the portion of the hysteresis loop in the second quadrant (fig. I-8). To obtain the point of maximum product or $(BH)_{max}$, the analysis of a plot $BH(H)$ is the best way

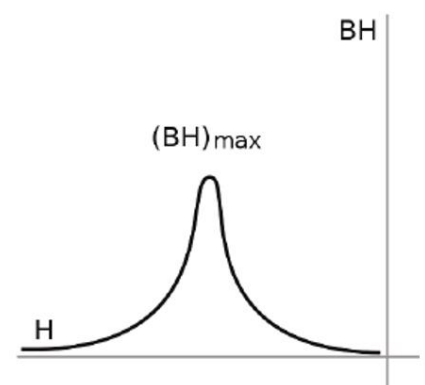


Figure I-8: $B(BH)$ plot, used to find $(BH)_{max}$

(figure I-7). This data gives us an idea of the energy a magnet can store. In table 2 the properties of few common permanent magnets are presented.

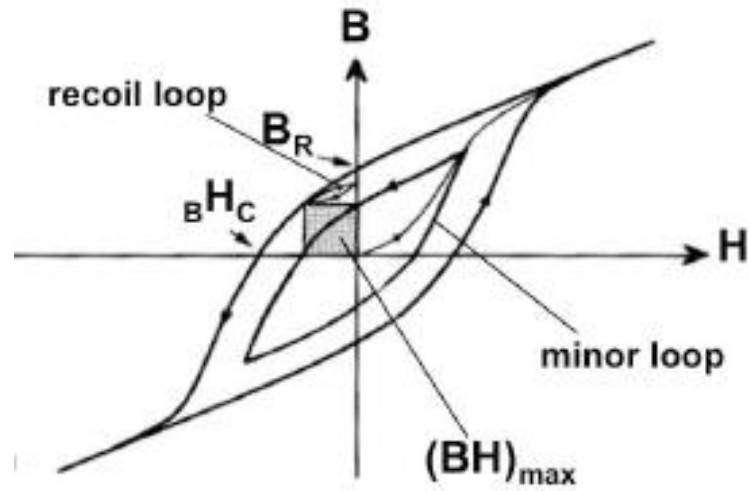


Figure I-8: Hysteresis loop showing where to find the energy BH .

Table I-2: Different value of the remanence, coercivity, Curie temperature and theoretical BH product for widely used magnets

Magnet	$\mu_0 M_R [T]$	$\mu_0 H_C [T]$	$BH_{max,th} [kJ/m^3]$	$T_C [K]$
NdFeB	0.7-1.3	1.0-2.8	514	585
SmCo	0.8	1.0-3.5	220	1000
FePt	0.7	1.0	407	750
AlNiCo	1.2	0.1	44	1200
Ferrites	0.4	0.3	29	720

3. Property and definition of coercivity

This is the coercive field which classifies magnetic materials into magnetically “hard” or “soft” materials. And the magnetic anisotropy is the parameter which governs coercivity. This anisotropy means that it exists energetically preferred directions for magnetization either related to the macroscopic shape of the sample (shape Anisotropy) or related to the crystalline axes (magneto-crystalline Anisotropy). The easy axis corresponds to the lower energy state and the one corresponding to higher energy is the hard axis..

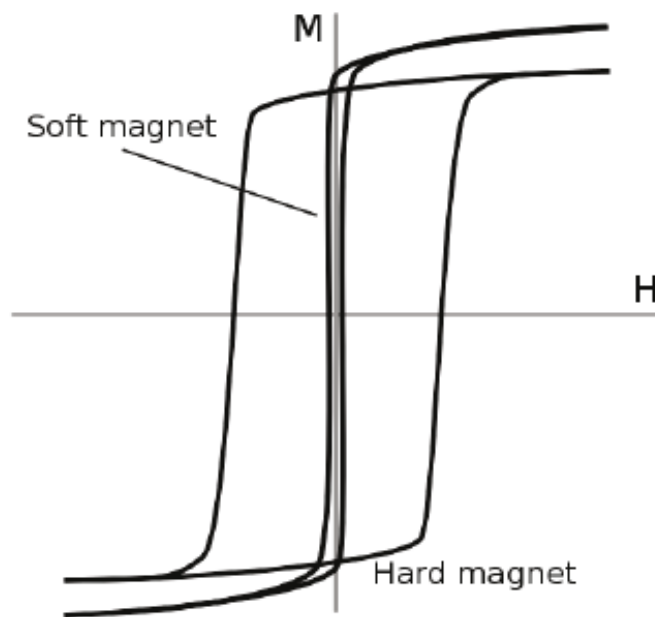


Figure I-9: Hysteresis loops for two magnets, one soft, with low coercivity, and one hard, with high coercivity. Both magnets present the same remanence.

Before explaining in detail the coercivity, it is important to explain the Stoner-Wohlfarth model, developed by Edmund Clifton Stoner and Erich Peter Wohlfarth and published in 1948. (2) It is the simplest model which describe the physics of fine magnetic grains containing single domains and where magnetization state changes by rotation or switching (abrupt reversal). In this model, the magnetization does not vary within the ferromagnet, and is represented by a vector \vec{M} . This vector rotates depending on the magnetic field H. The field is only varied along a single axis (usually the easy axis). The expression of the energy in general case is:

$$E = K_i V \sin^2(\theta - \varphi) - \mu_0 M_s V H \cos\theta$$

Where H is the applied magnetic field, M_s is the spontaneous magnetization, and V the volume of the magnet, and μ_0 is the vacuum permeability.

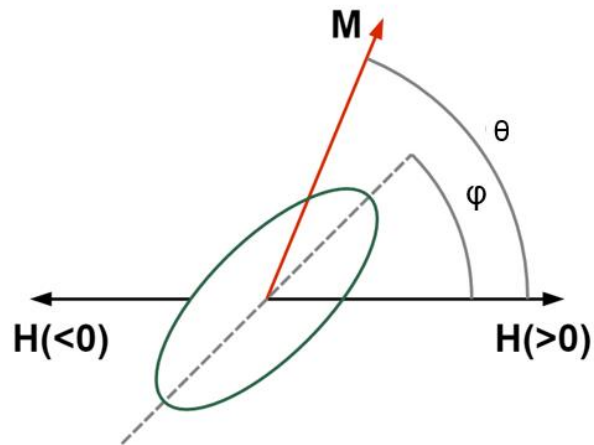


Figure I-9: Draw of a particle under a magnetic field H , the magnetization M , and the easy axis in dashed line

In uni-axial systems, there is only one easy axis and the anisotropy energy density is approximated to:

$$E(\theta) = K_1 \sin^2\theta + K_2 \sin^4\theta + K_3 \sin^6\theta + \dots$$

Where K_i is the i^{th} order anisotropy (constant) and θ is the angle between the magnetization and the easy axis. Usually, only the first term is considered, except at low temperature. So, when in the reduced expression of (1.1) $K_1 > 0$, it exist two energy minima present of same energy, for $\theta = 0$ and $\theta = \pi$ (cf. Fig. 1-9). This leads to the magnetization alignment along the z easy-axis, with a positive or negative orientation.

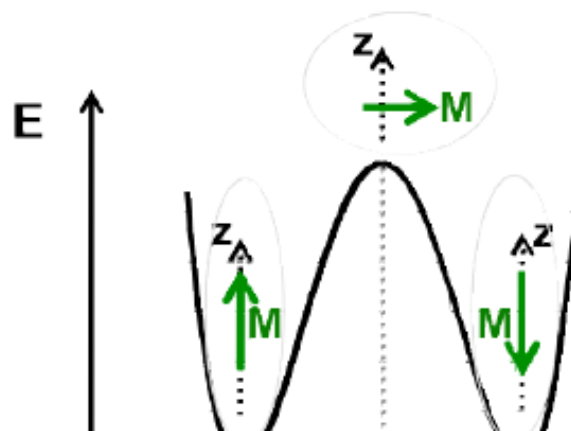


Figure I-10: Schematic of the energy barrier in the case of a uni-axial system with no external applied magnetic field.

Without external magnetic field, the system will occupy one of the two possible states with equal probability.

The maximum energy at $\theta = \pi/2$ corresponds to the hard axis, and the energy is the one needed to align the magnetization in a perpendicular direction to the easy axis. This energy is called the anisotropy energy, and is responsible for the value of coercivity and existence of remanence. If we consider now that the magnetization is aligned along the easy axis at $\theta = 0$ and a magnetic field is applied along the same axis, at $\theta = \pi$. The associated energy of Stoner-Wohlfarth model becomes:

$$E(\theta) = K_1 \sin^2 \theta + \mu_0 M_s H \cos \theta$$

The energy profile changes in:

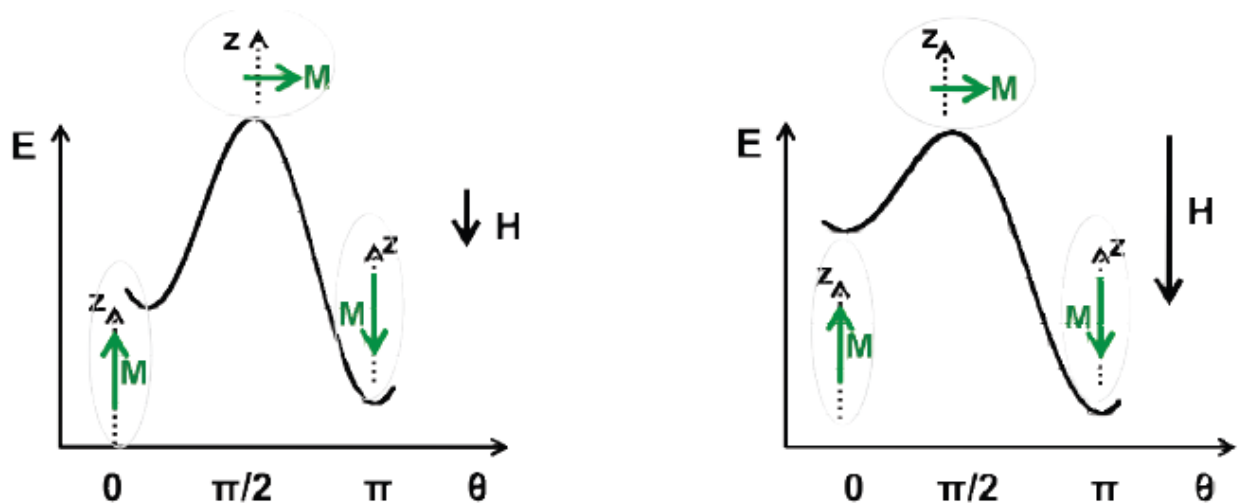


Figure I-11: Evolution of the energy barrier in the presence of an increasing magnetic field.

With the increase of the field strength, the energy state corresponding to the magnetization anti-parallel to H ($\theta = 0$) is raised while the one parallel to H ($\theta = \pi$) is lowered (cf. Fig. 1-10). At high magnetisation, when $H \geq H_c$ the barrier between the state where $\theta = 0$ and $\theta = \pi$ disappears, then the magnetization flips and aligns along the applied field. In real systems, the coercivity is an extrinsic physical property. It depends on the material's anisotropy but also strongly on the material's microstructure.

However there are different types of magnetization reversal in uniaxial high anisotropy systems. Nucleation of the reversal implies the occurrence of instabilities

in the saturated magnetic state for a certain value of an applied field, H_N , the nucleation field. In the Stoner Wohlfarth model, $H_N = H_C$, in reality, there is the apparition of an effect of propagation which also contributes to the reversal. The larger of these two fields determines the value of the coercive field. But it exists two cases of nucleation, they will be described in the following paragraphs.

The first case, comes from the Stoner-Wohlfarth model, we can consider the magnetic moment parallel and the magnetization homogeneous at any moment (valid only for small particles). In this case, called coherent rotation, when the field is applied along the easy axis, the coercive field, identical to the nucleation field, is equal to the anisotropy field. To reverse the direction (from one easy axis to the other), the magnetization does not change the magnitude and it has to pass through the hard axis. Then to arrive at the next position, it must to pay the anisotropy energy to arrive to its

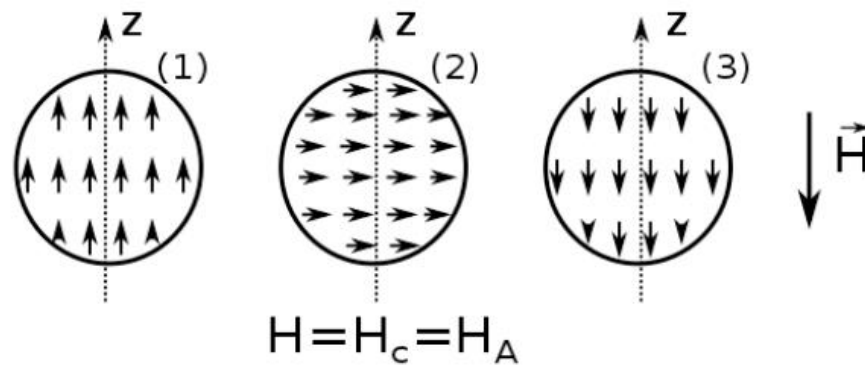


Figure I-12: Schematic representing coherent rotation in uni-axial systems.

next position of low energy. (cf. figure 1-11). The value of the anisotropy field in this case is:

$$H_N = \frac{2K_1}{\mu_0 M_s}$$

Another type of magnetization nucleation is called magnetization curling. At the opposite of Stoner-Wohlfarth model, the magnetization does not stay homogeneous during the rotation. The magnetostatic energy reduces due to the apparition of flux closure. Then, this earn in energy compensates the payment of the exchange energy, unlike in the case of coherent rotation where the exchange energy was ignored. For the curling magnetization, the value of the nucleation field is:

$$H_N = \frac{2K_1}{\mu_0 M_s} - NM_s + \frac{cA}{\mu_0 M_s R^2}$$

The three terms involved are: A is the exchange constant, R is the radius of the ellipsoid and c is the constant that depends on the demagnetizing factor N, of value 8.666 for spheres and 6.678 for long cylinders.

In the case of high anisotropy, the difference between coherent rotation and curling is minor. Nevertheless, the experimental value of coercivity is always smaller than the one calculated from the two previous cases. This phenomenon can be explained by the fact that the micro/nanostructure has a strong influence on the coercivity. The presence of low anisotropy areas in the material dramatically decreases the value of the coercive field. In these low anisotropy areas starts the nucleation, and then it will propagate in the entire system in contact with the region. Therefore, the presence of a defect can induce the reversal of the main part of the system. After nucleation, reversal can propagate in the entire system for the same field. Then we say that reversal is controlled by nucleation. If the nucleus remain pinned at magnetic heterogeneities, then we say that it is pinning controlled. The nucleus can also disintegrate spontaneously if the energy is

not enough to maintain it. Nucleation controlled materials, are essentially homogeneous in the bulk. The position of the nucleus does not influence the domain wall energy. The mechanism of pinning controlled materials is explained in figure 1-12. In (1) the direction of the applied field get reversed to lead to (2). In (2) the nucleation starts, the domain wall is formed and starts to propagate. At (3), the wall encounters some defect(s) and is pinned there. In order to unblock the wall and obtain saturation (4) in opposite direction, a higher field is needed.

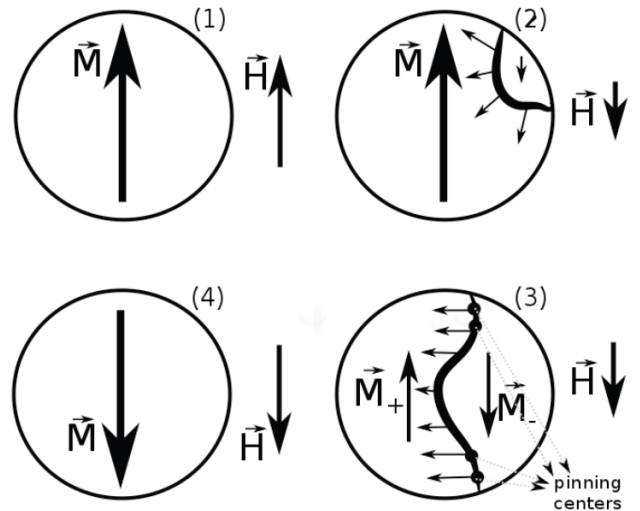


Figure I-13: Depiction of magnetization reversal in the case of nucleation pinning reversal mechanism.

B. Magnetic materials for permanent magnets

Permanent magnets are made of different materials: ferrites, rare-earth compounds, etc. Early magnets were based on natural material called loadstone. The main compound which is included into the content of loadstone is magnetite (Fe_3O_4). The first invention based on permanent magnet was made in China. Magnetite, carved in the shape of a Chinese spoon, was the first magnetic device “South pointer” (3). With time the concepts and the application of permanent magnets faced changes in XX century with the apparition of important discoveries. Figure I-15 represents the evolution of the energy product $(BH)_{\max}$ with the development of magnetic materials (4).

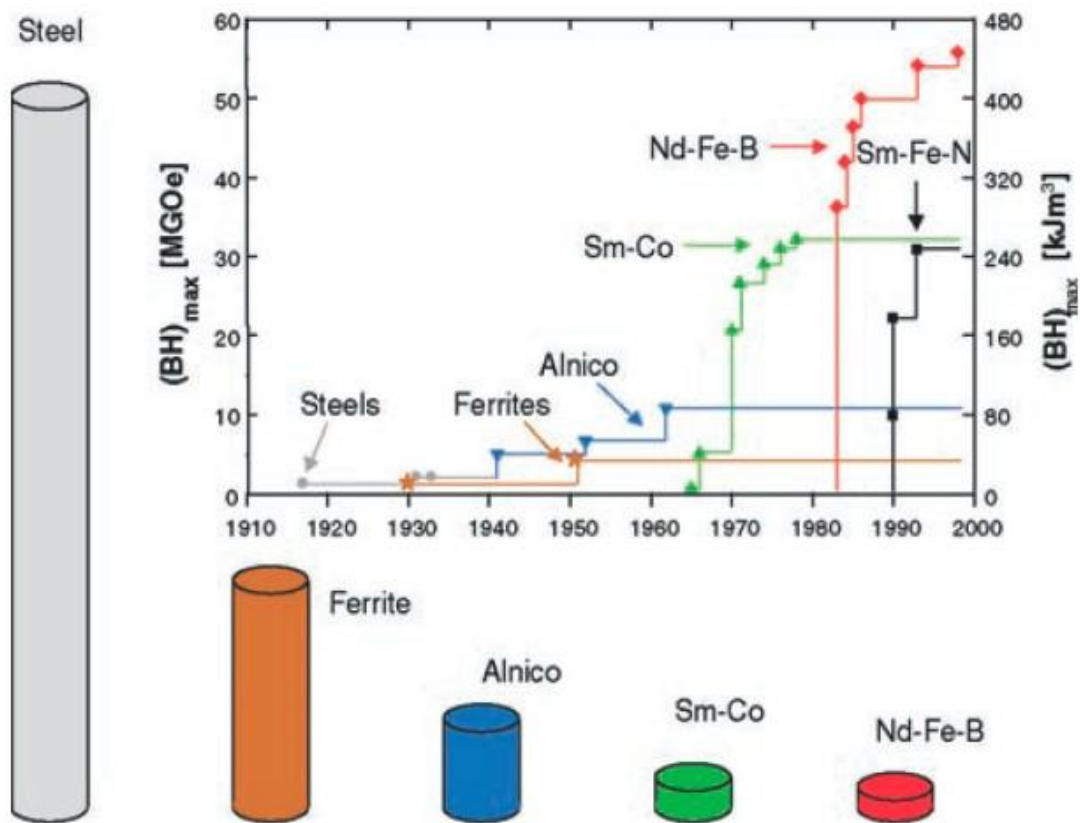


Figure I-14: Evolution of the energy product $(BH)_{\max}$ with the development of magnetic materials

This impressive increase of the efficiency of permanent magnets come from the discovery of magnetic materials with high properties. In the end of XIX century, iron-based tungsten steel magnets were discovered and in 1917 steel magnets based on cobalt were invented in Japan (5). One of the most important breakthroughs in hard magnetic materials was the invention in 1931 of the Alnico (aluminium–nickel–cobalt–

iron alloy). Alnico magnets have better properties than previous available steel magnets because of their strong shape anisotropy with two-phase nanostructures. FeCo particles are surrounded by an Al-Ni matrix weakly magnetic, which enhance the magnetic hardness. The next huge step in development of the magnetic materials was the elaboration of ceramic as permanent magnet in 1950 by Philips (6). Ceramic permanent magnets increased coercivity, but have relatively low Curie temperature and low magnetization. Another significant discovery was made in 1960s with the invention of rare-earth permanent magnet such as rare-earth-cobalt compounds. The difference between this rare-earth magnets and the previous one is the kind of magnetic anisotropy. Before the magnetic properties were mostly due to the shape anisotropy. The new generations of the rare-earth permanent magnet have their properties due to magneto-crystalline anisotropy. Magneto-crystalline anisotropy is an intrinsic property. The magnetization process is different when the field is applied along different crystallographic directions, and the anisotropy reflects the crystal symmetry. Its origin is in the crystal-field interaction and spin-orbit coupling, or else the interatomic dipole–dipole interaction.

The first generation of the high performance magnets was the SmCo_5 compound, it was the best material in the field of permanent magnets. Indeed SmCo_5 has larger coercivity and energy product than previous hard magnetic materials. SmCo_5 compound had the highest magneto-crystalline anisotropy, and therefore the highest theoretical coercivity could be obtain from the magnets based on this compound. Moreover, they also possess good thermal stability and their Curie temperature is still the highest (from 700 °C to 800 °C). These excellent intrinsic properties of SmCo_5 compound lead to use it in high-temperature applications. The second generation was rare-earth permanent magnet compound $\text{Sm}_2\text{Co}_{17}$ with the addition of small amount of Cu, Fe and Zr. Permanent magnets based on $\text{Sm}_2\text{Co}_{17}$ compound showed increased energy product due to the higher Co content and also excellent thermal stability (high Curie temperature). However, $\text{Sm}_2\text{Co}_{17}$ compounds have relatively low magneto-crystalline anisotropy.

The high price of Sm and Co led to an intense search of a Co free material, for example iron-based rare-earth compounds, with similar characteristics than Sm-Co materials. In 1984, a new iron-based rare-earth permanent magnet $\text{Nd}_2\text{Fe}_{14}\text{B}$ was reported by Sagawa et al and Croat et al (7). The intrinsic properties of the new Nd-Fe magnets were remarkably higher than the predecessors and the new Nd-Fe-B compounds were therefore called the third generation of rare-earth permanent magnets.

This new generation had a significant influence on the application in large scale for the past two decades. Nd-Fe-B magnets became the leading compounds on the permanent magnet market owing to their excellent magnetic properties at room temperature and their relatively low cost per energy-density unit. In 2011, the “rare-earth crisis” blew up, when China revised its politics regarding the prices and export of the rare earths (8). In fact, the origin of this crisis was not the lack of Nd and other light rare earths, which are not so rare in comparison with the other metals we use in a large quantity (e.g. Cu). The main problem is the lack of heavy rare earths (mainly Dy and Tb) which are widely used as dopants in permanent magnet of the third generation to improve the thermal stability. A significant amount of heavy rare earths, Dy and Tb, have to be added to this Nd-Fe compounds to improve their stability at temperatures above 100°C . Nowadays a lot of efforts are made to decrease the use of heavy rare earths in Nd-Fe-B magnets using different manufacturing techniques. In addition, the research works for new materials with the same or better intrinsic properties than the third generation are carried out.

As a result of intensive research, several new rare-earth-based alloys for permanent magnets have been synthesized. One on the good candidate for powerful permanent magnet is the Sm-Fe-N alloy. The $\text{Sm}_2\text{Fe}_{17}\text{N}_3$ has larger anisotropy field, higher saturation magnetization and higher T_C than Nd-Fe-B alloys (9). However, conventional sintering techniques are not suitable for elaboration of high performance Sm-Fe-N permanent magnets due to the degradation of the compound above 873K. At this temperature the magnetic $\text{Sm}_2\text{Fe}_{17}\text{N}_3$ phase decomposes into two paramagnetic phase α -Fe and SmN following the reaction:



The formation of these phases leads to a total loss of the magnetic properties of the PM (10). Nowadays, the main techniques to obtain Sm-Fe-N dense permanent magnet from powder are use of high pressure compaction, or binder and production of bonded magnets. However, the resulted magnetic performance of bonded Sm-Fe-N magnets is lower than the one of original Sm-Fe-N powder, mainly due to the existence of important amount of nonmagnetic binder. This highly restricts the application of Sm-Fe-N magnets and forces the research of new manufacturing technologies.

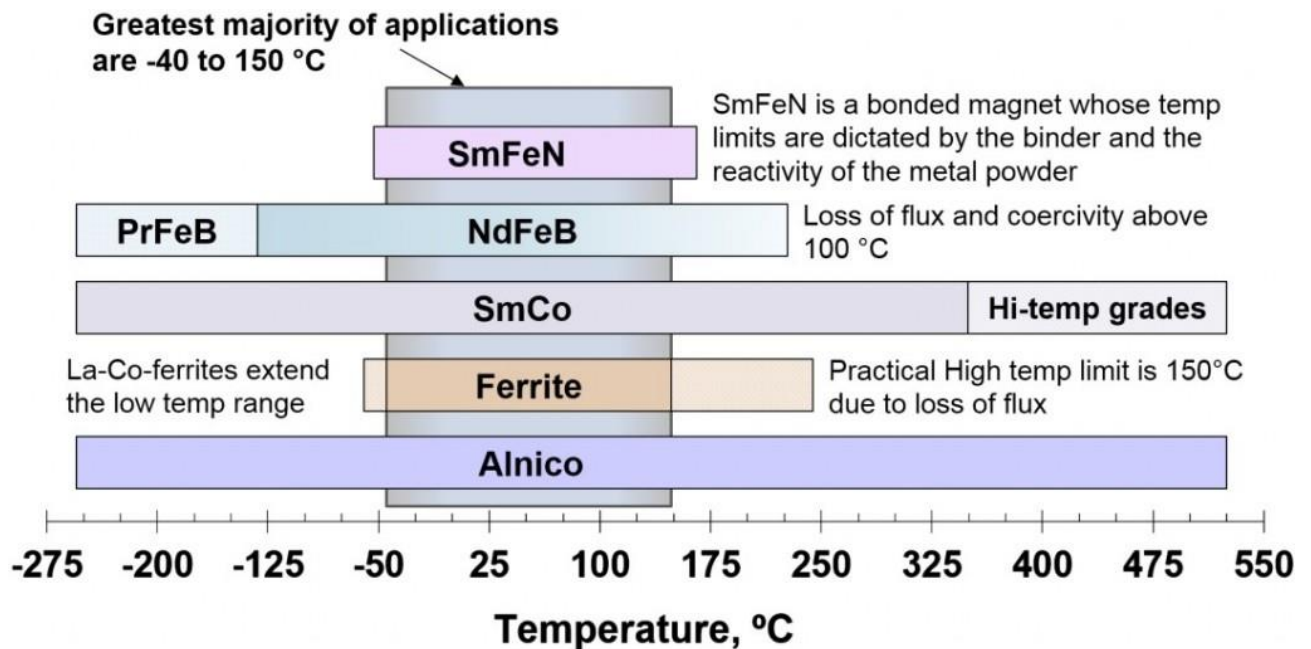


Figure I-15: Classification of magnets depending of the temperature dependence

II. Chapter 2: Elaboration and characterisation of Sm-Fe-N permanent magnet

A. State of the art

To obtain $\text{Sm}_2\text{Fe}_{17}\text{N}_3$ Schnitzke et. al. elaborated a method of synthesis using mechanical milling of $\text{Sm}_2\text{Fe}_{17}$ to decrease the size of the powder ($<50\mu\text{m}$) and then under NH_3/N_2 (1:2) during 2h at 450°C to obtain $\text{Sm}_2\text{Fe}_{17}\text{N}_3$. Finally, the product obtained is ground in a vibrating mill to obtain a grain size $<3\mu\text{m}$.

1. Sintering of $\text{Sm}_2\text{Fe}_{17}\text{N}_3$ by non-conventional techniques

Many different techniques of sintering and compaction have been used and studied to improve the density and the homogeneity of this material with a temperature below 500°C to avoid SmN and αFe formation.

Hu et. al. worked on explosion sintering and grain size influence (also Kurima Kobayashi, (11)) on coercivity and densification. (12) This study shows a great amelioration of the density via this method of sintering which use high pressure, with a density up to $7,4\text{g}/\text{cm}^3$. Also the study on the grain size, gives interesting results for this compound. Indeed, usually with a decrease of the grain size, the densification increase, but according to this study, if the size increases ($\langle l \rangle = 1\mu\text{m}$ to $\langle l \rangle = 5\mu\text{m}$), then the density is better. Also during the coercivity analysis with different size of grain, the results show that with smaller grains, the coercivity is improved.

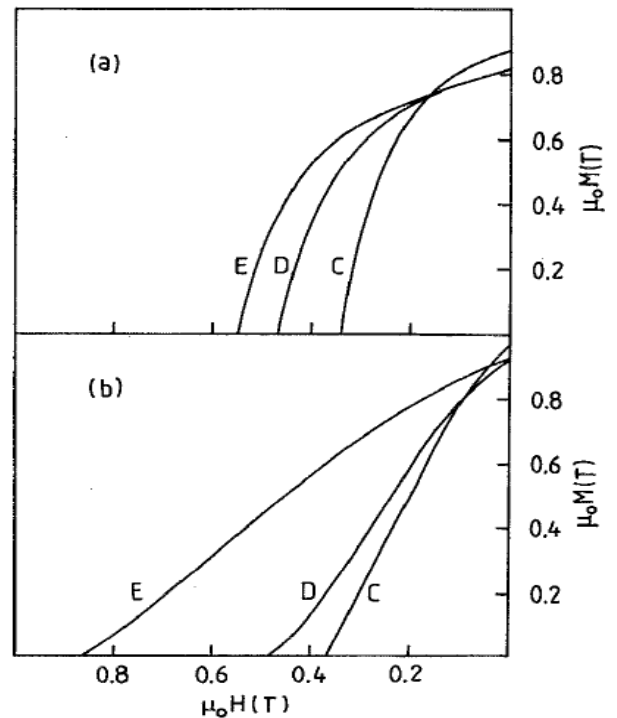


Figure II-1 Coercivity observed for different grain size. Top for sintered and down for powder. E- $1\mu\text{m}$ D- $2\mu\text{m}$ C- $5\mu\text{m}$ (12)

Machida et. al. studied this alloy with a compaction of 3GPa, and for different temperature, and compared to previous studies. (13) He shows that the high pressure does not affect the remanence, but decrease the coercivity. Also the best result obtained for 3GPa is sintered at 550°C as shown in the table. This sample has a density of 7,77g/cm³, which is very close from the theoretical one. Also the magnetic properties measure and XRD analysis show a low concentration of SmN and α Fe, and then non effect on the magnetism. This study is very promising, but have a major problem, the high pressure it require.

Tsutomu Mashimo et. al. have been able to obtain very dense pallet (7,3-7,6 g/cm³) using a first pressing a 100MPa and the shock compression technique. This

Compound	Treatment			Density (g/cm ³)
	<i>P</i> (GPa)	<i>T</i> (°C)	<i>t</i> (min)	
Sm ₂ Fe ₁₇ N _{3.8}	3	300	30	7.99
Sm ₂ Fe ₁₇ N _{3.7}	3	550	30	7.77
Sm ₂ Fe ₁₇ N _{3.8}	3	800	30	8.11
Sm ₂ Fe ₁₇	7.98 ^a
Sm ₂ Fe ₁₇ N ₂	7.68 ^a
2SmN + 17 α -Fe	8.11 ^a

^aThese density values are calculated from the lattice parameters reported on Sm₂Fe₁₇ (Ref. 12), Sm₂Fe₁₇N₂ (Ref. 12), SmN (Ref. 13), and α -Fe (Ref. 13), respectively.

Table II-1: Densities obtain for different temperatures of sintering under high pressure (13)

technique enable to use high pressure (here 7-12 GPa) and use special die, called capsules, made in this case with Al. (14)

Magnetic pre-alignment is often use to improve the magnetic properties with a SPS process, and as shown by Saito et. al. it leads to good results on the remanence. (10) Magnetic pre-alignment of the powder is done before SPS process and direction of applied magnetic field is perpendicular to the pressure in SPS.

To resume, the conditions to obtain a dense material (necessary condition to obtain good magnetic properties) are extreme and can't be produce in an industrial way. Indeed this kind of compaction only work for small objects, and then could not be use in the elaboration of motor.

2. Use of binders

In order to avoid to use extreme process of compaction, the use of binder is necessary. In this case, the use of magnetic element is helpful, because it allow use to use a significant amount of it without an important decrease of the searched properties. This is why Zn have been chosen, with a low melting point (419°C) it is a good candidate as binder. (9) (15) Even if in the literature other elements have been used (Co, Fe,), because the studies carried out in our laboratory are about Zn, we will focus on this binder.

In a first place, this binder (in a fraction of 5-15wt %) allow a good densification 6.9 g/cm^3 at small temperature of sintering (400°C) (9). But also an increase of the magnetic properties, especially the coercivity. Also the addition of Zn avoid the formation of αFe by the formation of the non-magnetic phase FeZn_4 . It have been suggested than the reduction of deterioration retard the decrease of coercivity. By the use of SPS, very good results have been found, such as 2,75T of coercivity and 0,62T of remanence after annealing with a temperature of 435°C during 1h under 600MPa.

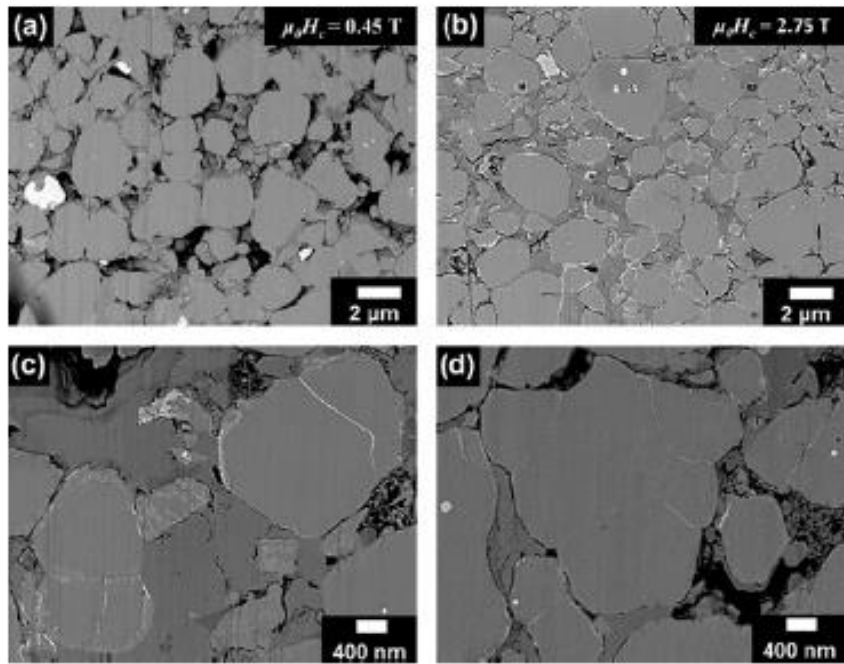


Figure II-2-1: Low-magnification SEM BSE images of (a) as-sintered (low coercivity) and (b) post-sinter-annealed (high coercivity) samples (coercivity values are shown in the inset). Relatively high-magnification images of the post-sinter-annealed sample showing the formation of (c) particle boundary and (d) grain boundary phase. (9)

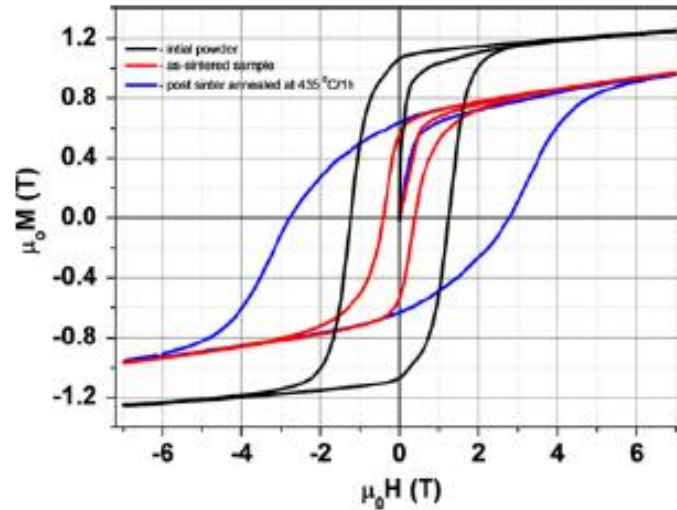


Figure II-2-2: Magnetic hysteresis loop of the initial powder (black line), as-sintered (red line) and post-sinter-annealed bulk sample (435 °C/1 h) (blue line) (9)

It is then shown that the use of this binder is efficient for this material, and can lead to a great magnetic composite material.

B. Description of the techniques

1. The Spark Plasma Sintering (SPS) technique

The sintering is a process taking part in the realisation of ceramics. Macroscopic effect of the process is the volume shrinkage and the strengthening. It is a thermal treatment for bonding particles into a coherent and predominantly solid structure, via mass transport events that often occur on the atomic scale. The force acting in this process is surface energy reduction. The bonding leads to improved strength and a lower system energy. On the figure II-3 we can see the different steps during the sintering and the apparition of the grain boundaries. To define mathematically the process, the instinctive approach would be to work on the coalescence of viscous particles driven by surface tension (made by Frenkel in 1945), which leads to the relation:

$$-\frac{\partial E_s}{\partial t} = 2\eta\dot{\epsilon}^2V$$

Where E_s is the surface energy, and V the volume deformation, $\dot{\epsilon}$ is the strain rate, and η the density.

However, the other approach which appears to be the best one to describe this phenomenon, is the evaporation of emptiness (made by Pines in 1946), which leads to:

$$C = C_0\left(1 - \frac{2\alpha}{r} \frac{\Omega}{kT}\right)$$

Where, Ω is the atomic volume, C the concentration C_0 the concentration for $t=0$ min, r the pore radius, and α the surface tension.

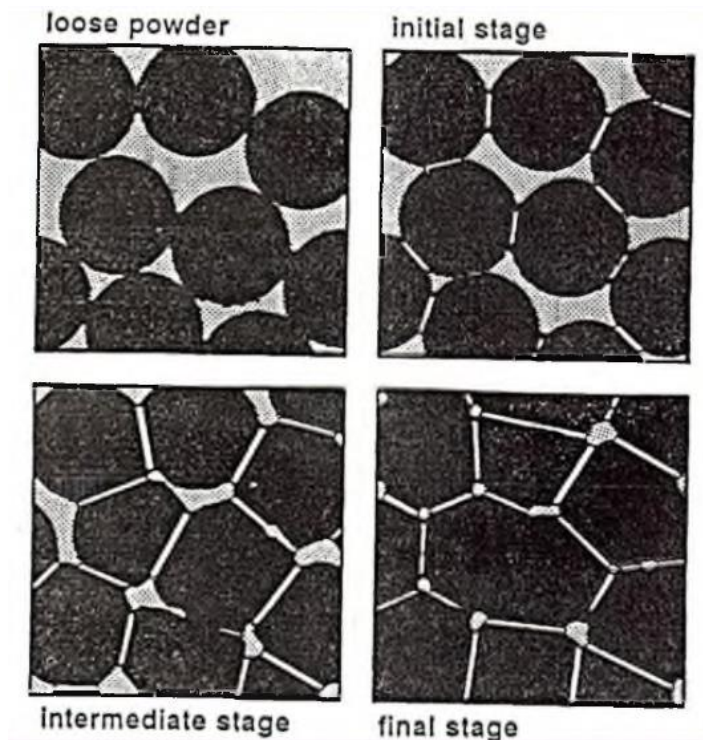


Figure II-3: Representation of the grain growth and the formation of the gain boundary in the four stages. Loose, initial, intermediate and final stages.

In practice for conventional sintering, the powder is compressed via a press to obtain a green body, then the object is placed in an oven and heated at a determined temperature. To rise the wanted temperature, the oven (at $t=0\text{min}$; $T=T_{\text{ambient}}$) use few temperature's step.

However, the Spark Plasma Sintering is an unconventional technique of sintering. It is important to say than in SPS, there is not apparition of sparks or plasma. (16) This is an emerging powder consolidating technique, which provides potentially revolutionary capabilities to the processing of materials into configurations previously unattainable. SPS consists essentially of the conjoint application of high temperature, high axial pressure and electric current assisted sintering. (See figure II-4)

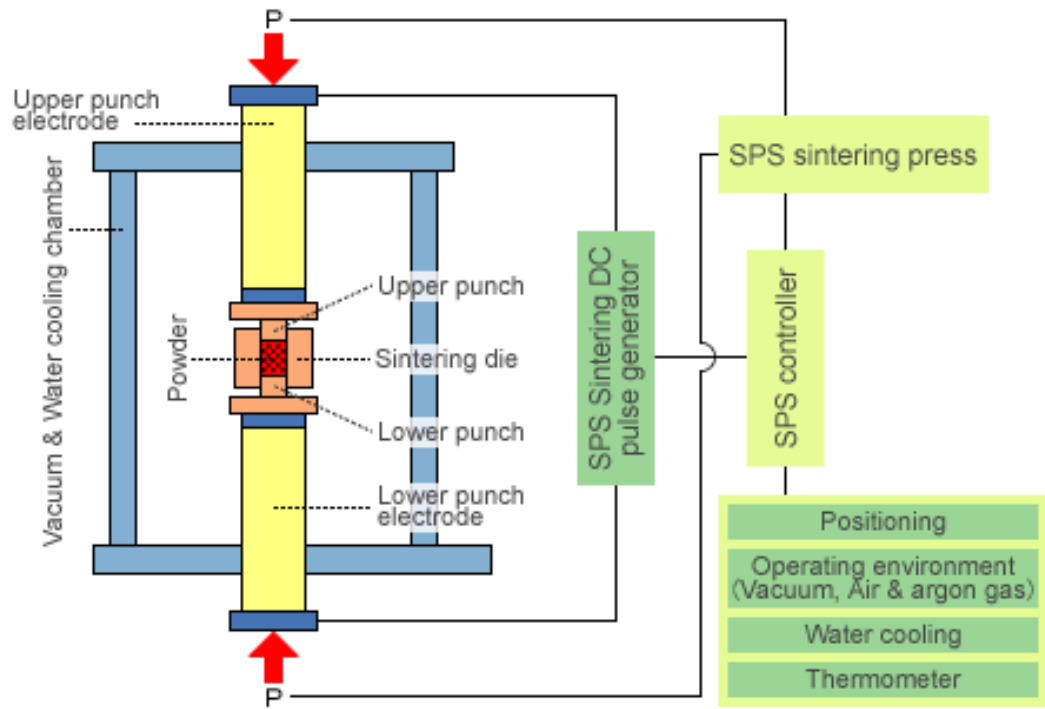


Figure II-4: Schema of the SPS device, including, the press, the controller, and generator.

The fact of having an electric current passing through the die and the power while applying the pressure create a Joule effect, which increase the temperature on the grains' necks, which help to the matter diffusion and the neck growth. It give us better compaction's results. So this results provide from the enhancement of the matter displacement, which come from a thermal and field effects.

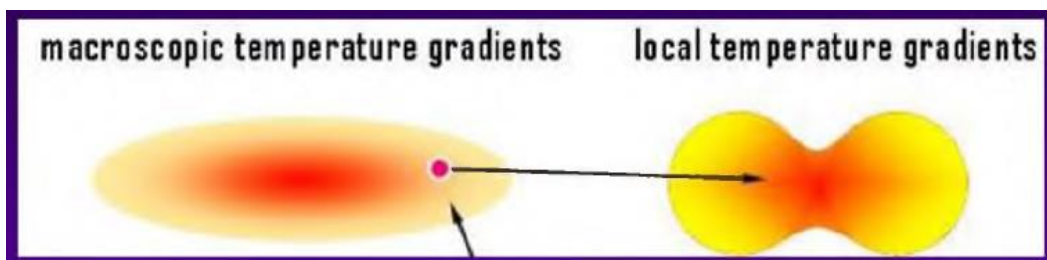


Figure II-5: Temperature gradients in macroscopic view, and local view. In local view we can see the increase of the temperature on the part of the neck.

2. X-Ray Diffraction (XRD) analysis

X-ray powder diffraction analysis (XRD) is one of the most used analytical techniques for characterizing materials. In this technique, the sample is usually used as powder, (little grains of crystalline material). In the powder, the crystalline domains are randomly oriented. Therefore when the 2-D diffraction pattern is recorded, it shows concentric rings of scattering peaks corresponding to the different spacing in the crystal lattice. The positions and the intensities of these peaks are used for identifying the underlying structure (or phase) of the material. For example, the XRD of graphite is different from diamond even if they both are made of carbon atoms. When a focused X-ray beam interacts with a planes of atoms, there is 4 different interactions:

- a part of the beam is transmitted,
- a part is absorbed by the sample,
- a part is refracted and scattered,
- and finally a part is diffracted.

Diffraction of an X-ray beam by a crystalline solid is similar to diffraction of light by a prism, producing a rainbow. X-rays are diffracted by each mineral differently, depending on what are the elements which make up the crystal lattice and the configuration of these atoms. When an X-ray beam hits a sample and is diffracted, we can measure the distances between the planes of the atoms that constitute the sample by applying Bragg's Law:

$$n\lambda = 2d \sin\theta$$

Where the integer n is the order of the diffracted beam, λ is the wavelength of the incident X-ray beam, d is the distance between adjacent planes of atoms (the d-spacing), and θ is the angle of incidence of the X-ray beam. Since we know λ , and we can measure θ , we can calculate the d-spacing. The X-ray scan provides a unique "fingerprint" of the mineral or minerals present in the sample. When properly interpreted, by comparison with standard reference patterns. Usually, X-rays are

generated with a tube under vacuum. A current is applied that heats a filament in the tube; the higher the current the greater the number of electrons emitted from the filament. A high voltage accelerates the electrons, which will hit a target, commonly made of copper. When these electrons hit the target, X-rays are produced. The wavelength of these X-rays is characteristic of that target. These X-rays are collimated and directed onto the sample. A detector detects the X-ray signal; the signal is then processed either by a microprocessor or electronically, converting the signal to a count rate. Changing the angle between the X-ray source, the sample, and the detector at a controlled rate between settled limits is an X-ray scan. Applications XRD analysis has a wide range of applications in material science, chemistry, geology, environmental science, forensic science, and the pharmaceutical industry for characterizing materials.

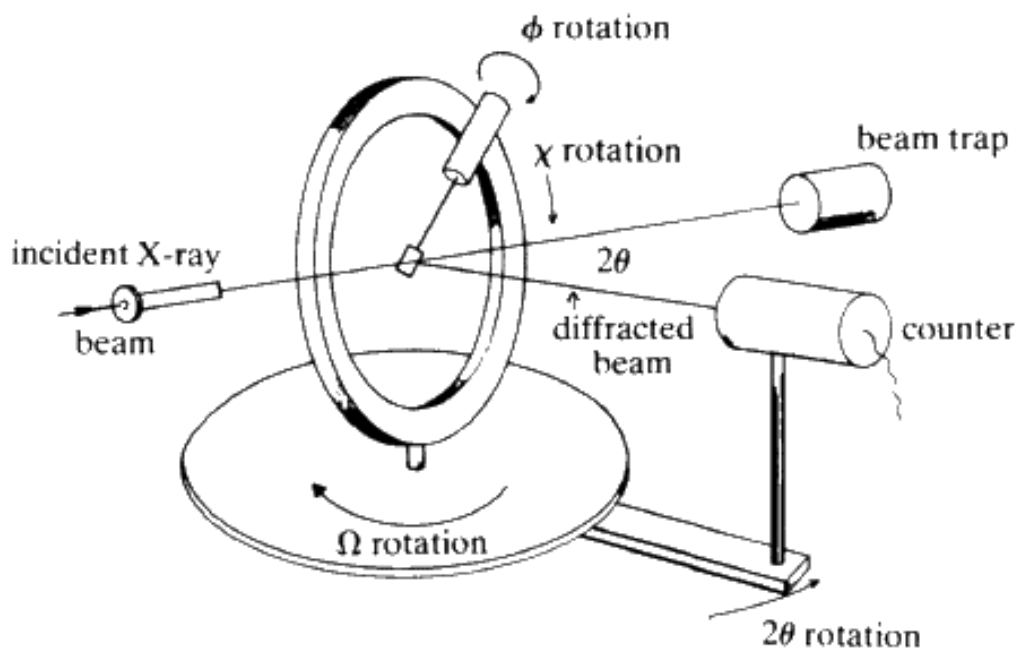


Figure II-6: General scheme of a X-Ray diffractometer.

3. Scanning Electron microscopy (SEM)

The Scanning Electron Microscope is made of three main part: The canon, where the electron beam is produced, the chamber, where is disposed the sample, and the sass to communicate with the outside. The use of SEM needs an important vacuum, around 10^{-10} Pa in the canon and 10^{-6} in the chamber. The emission of the beam is obtain using a high current through a filament, which produce a thermos-ionic emission of electrons. As for the XRD, we use high voltage in order to increase the number of pulled off electrons. However, the electrons does have the same direction and speed, we need to focalise them. For that we have multiple lenses and diaphragms, having adjustable focal distances, and opening. The electron beam pass through the lenses, and arrive on the sample. There, the emitted electrons (called primary electrons) will, penetrate in the matter and pull of the surface electrons of the target in a define zone around the impact point of the beam (10-20nm). These last electrons are called

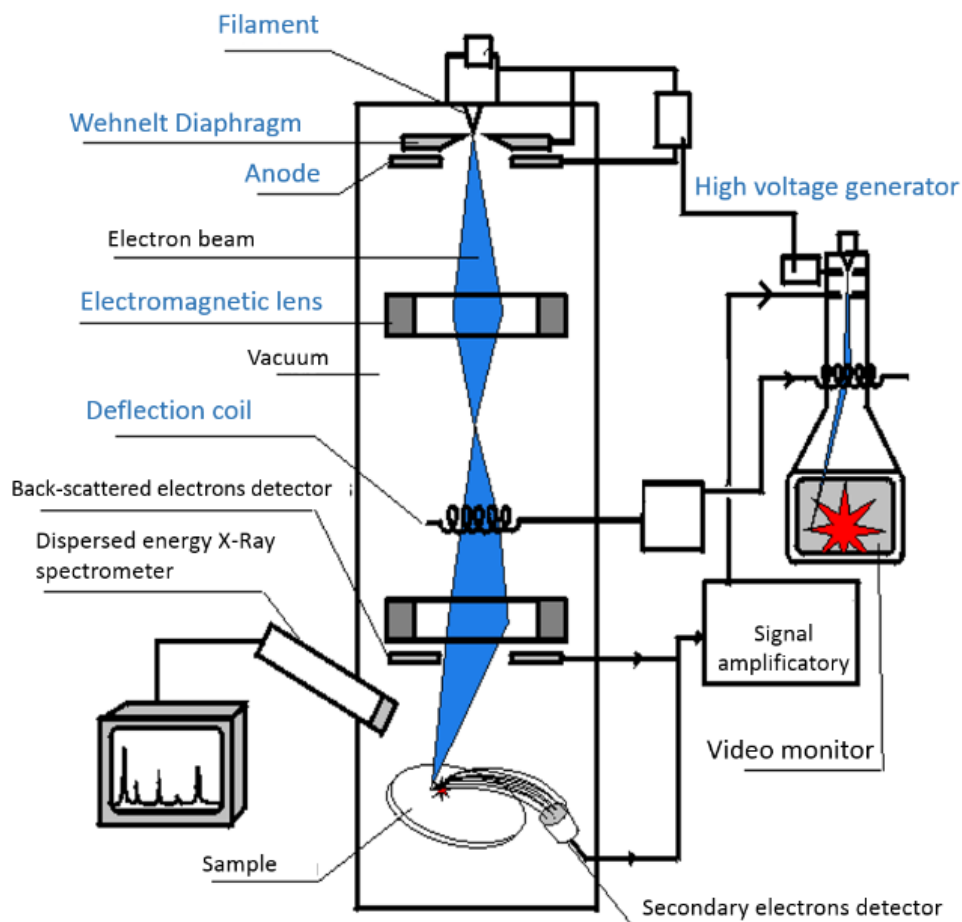


Figure II-7: Scheme of the composition and the functioning of a Scanning Electron Microscope

secondary electrons, and will strike on the detectors. With this detection we obtain an effect of relief because of the angle between the detector and the sample, but the SEM is then limited in resolution by the width of the electron diffusion in the sample, which depend of the opening of the diaphragm. Another way to observe the sample is to look the back-scattered electrons. For that, a detector is disposed just under the first lenses and the electrons which pass next to a nucleus a refocuses just above the first lenses. It is with this detector that we obtain the best resolution.

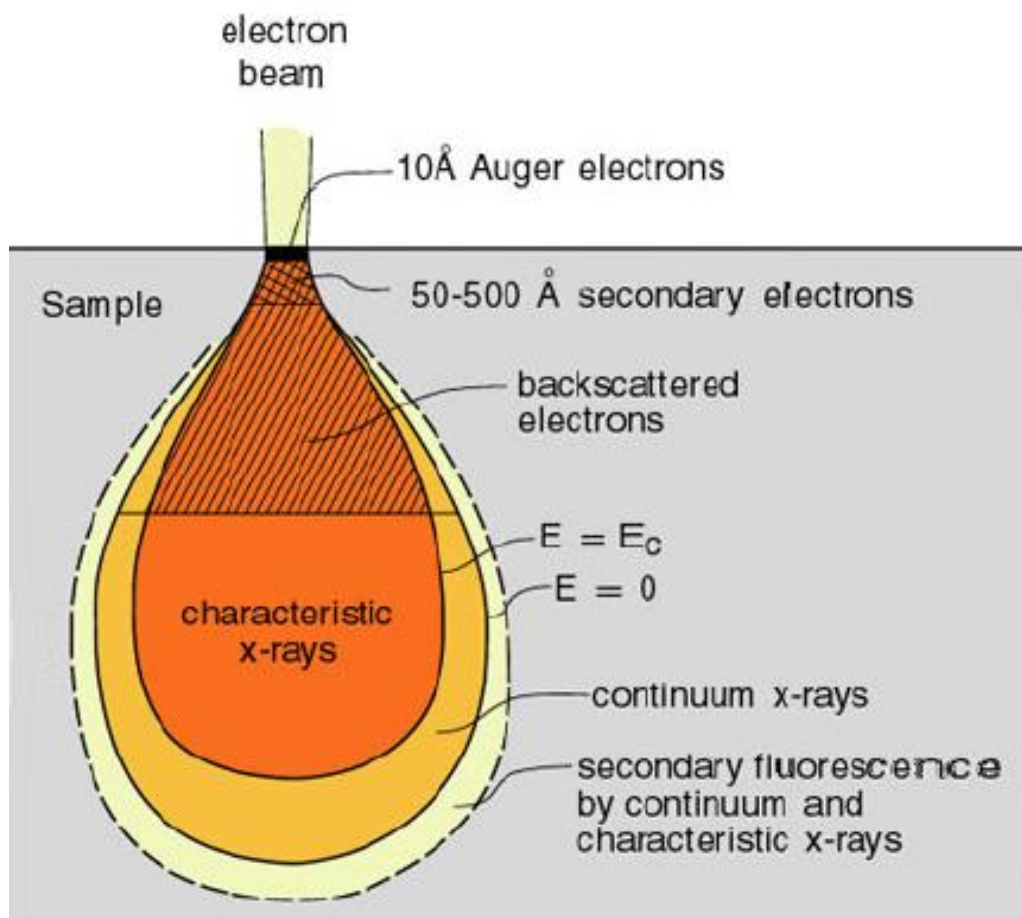


Figure II-8: Representation of the interaction of electrons with the surface, and the interaction observed with a SEM.

The SEM can be used to make energy dispersive X-ray spectrometry (EDX). This spectrometry allows to make an elemental mapping of the object, to know where each elements is. Backscattered electrons and X-rays are generated by primary electron bombardment (electron beam). The intensity of backscattered electrons can be

correlated to the atomic number of the element within the sampling volume. Hence, some qualitative elemental information can be obtained. The analysis of characteristic X-rays (EDX or EDS analysis) emitted from the sample gives more quantitative elemental information. Such X-ray analysis can be confined to analytical volumes as small as 1 cubic micron.

4. Extraction magnetometry

Magnetometers are devices used for two purposes:

- To measure the magnetization of magnetic material like a ferrimagnet;
- To measure the strength and the direction of the magnetic field.

Invented in 1833 by C. F. Gauss, they are widely used in geophysics to measure the magnetic field of Earth and to detect magnetic anomalies. Because it can be used to detect submarines, some countries, (such as United States, Canada, and Australia) consider the most sensitive magnetometer as military technology. It can also be used as powerful metal detector (only works with magnetic metal), but the newest utilisation is, hen miniaturized, is as a compass in mobile phone and table computers.

But for laboratory research, the main use is to analyse magnetic properties of samples. There are many different kinds of magnetometers:

- SQUID (Superconducting quantum Interference Device), they work usually between 0,3K and 400K, with a magnetic field up to 7T. But they a noise sensitive, which make their utilisation incommode.
- Inductive Pickup Coils, measure the magnetization by detecting the current induced in a coil due to the changing magnetic moment of the sample.
- VSM (Vibrating Sample Magnetometer), makes the sample vibrating inside of a pickup coil, or a SQUID. The induced current or changing flux is measure and related to the magnetization. When combined with SQUID it appears to be more sensitive than either one alone.
- And others.

		σ (Sensitivity) A.m ²	 K	 Max. Tesla	 Rem. Oe.	 V sample Dim. in mm	 AC freq.	 Hydrostatic pressure	
Commercials equipments	 MPMS SQUID XL	5.10 ⁻¹¹	1,8 to 400		± 7	≈ 5	Ø5 x 5	0,1 Hz to 1 kHz	1,25 GPa
	 MPMS 3	5.10 ⁻¹¹	1,8 to 400	300 to 1000	± 7	≈ 30 Mini 5	Ø5 x 5		
	 VSM Oxford	5.10 ⁻⁸	Room T°		± 8		Ø5 x 5		
Laboratories equipments Extraction magnetometers	 BS1	5.10 ⁻⁶		200 to 850	± 7	≈ 30	Ø4,5x5		
	 BS2	2.10 ⁻⁶		1,6 to 330	±10,5	≈ 30	Ø6x6		
	 Magnetostriktion for bulk samples	ΔM		K	 Max. Tesla	 Rem. Oe.	 L sample mm	α Degree	
		10 ⁻⁷	3 to 300	6,3	≈ 5	2 to 8,8	360 d α = 1		

Figure II-9: Different type of magnetometer, (commercial, and laboratory) and their different capacities.

The Extraction magnetometer unlike in the VSM, the sample is fixed in the middle of an electro-magnet. This magnet produces an adjustable and uniform magnetic field H_0 . Another excitation, with lows amplitude in front of H_0 but with high frequency H , is overlaid. Because of the high frequency and the low amplitude of H , it does not effect on the position of particles. The field H leads to a variation of the induction in the sample. This induction is measured with a coil concentric to the sample. The value B/H gives a direct access to the differential permeability of the material for a static field H_0 (cf. figure II-10).

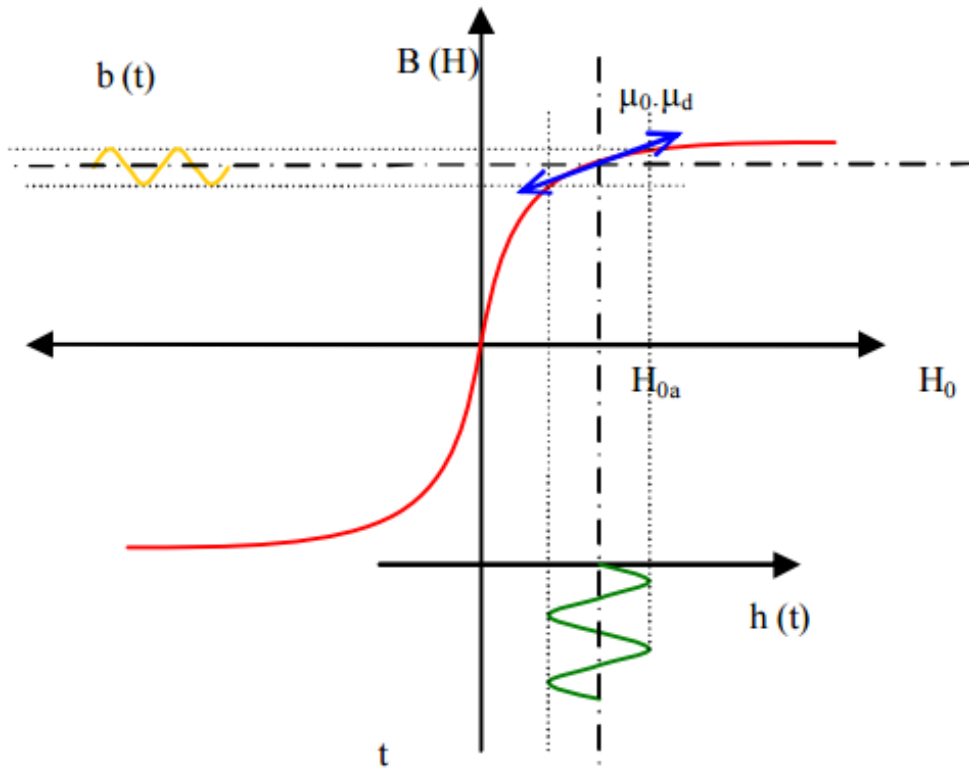


Figure II-10: Graph showing the principle of measurement of an extraction magnetometer

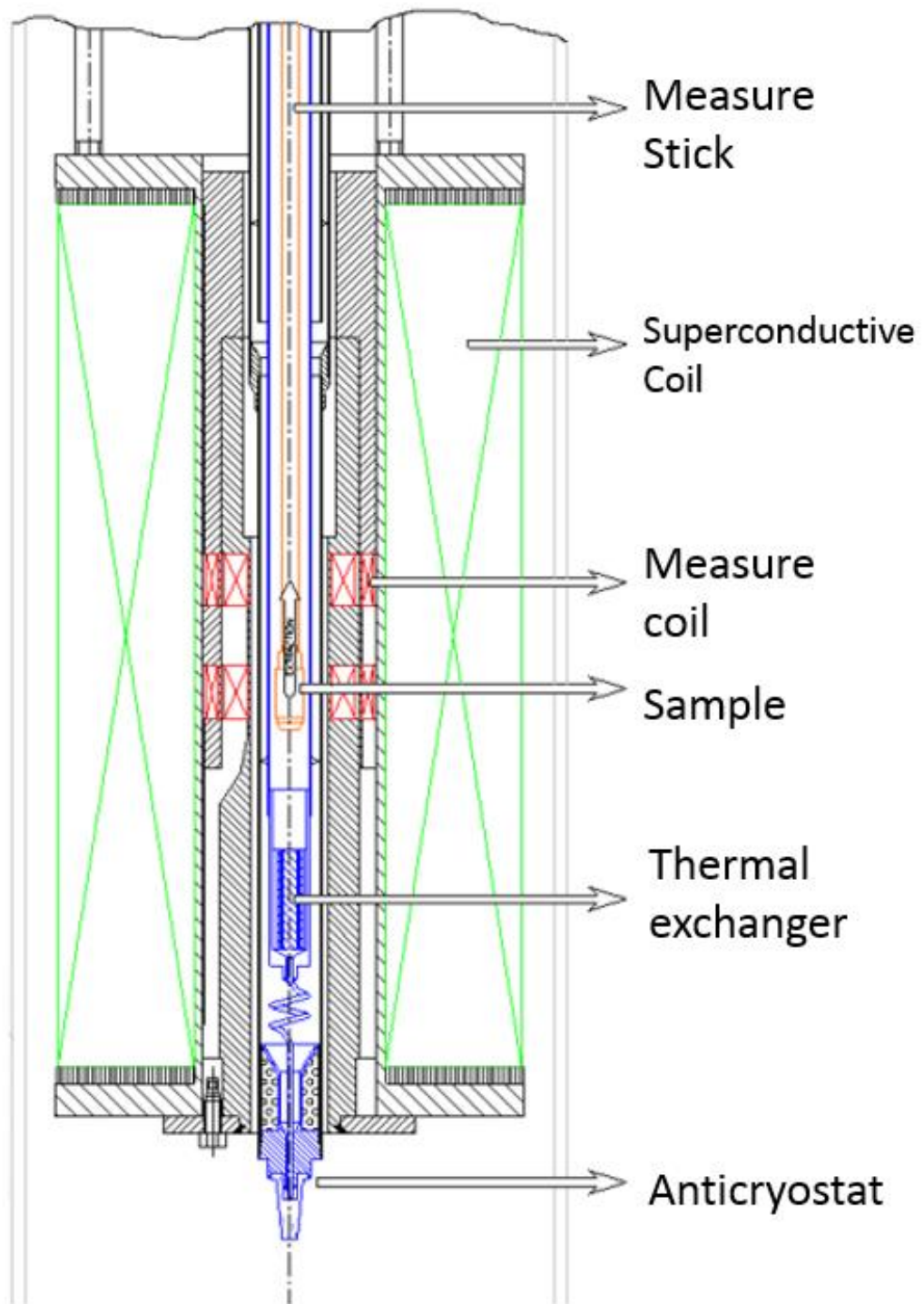


Figure II-11: Scheme of an extraction magnetometer

III. Chapter 3: Experimental procedure

A. Powder preparation

The $\text{Sm}_2\text{Fe}_{17}\text{N}_3$ powder have been produced and delivered by Nichia Corporation. The magnetic properties are reported in table III-1.

Tableau III-1: Magnetic properties of the $\text{Sm}_2\text{Fe}_{17}\text{N}_3$ provided by Nichia Corporation

Br	T	1,26
	kG	(12,6)
iHc	kA/m	1114
	kOe	(14,0)

Because of the presence of aggregate, the difficulties to disperse the powder, and the lack of the reflexion coefficient, the SALD analysis do not provides suitable information. Then, to obtain information of the size repartition we use a SEM, see figure III-1. This is how we know that we have particles ranging from 1 μm to 5 μm .

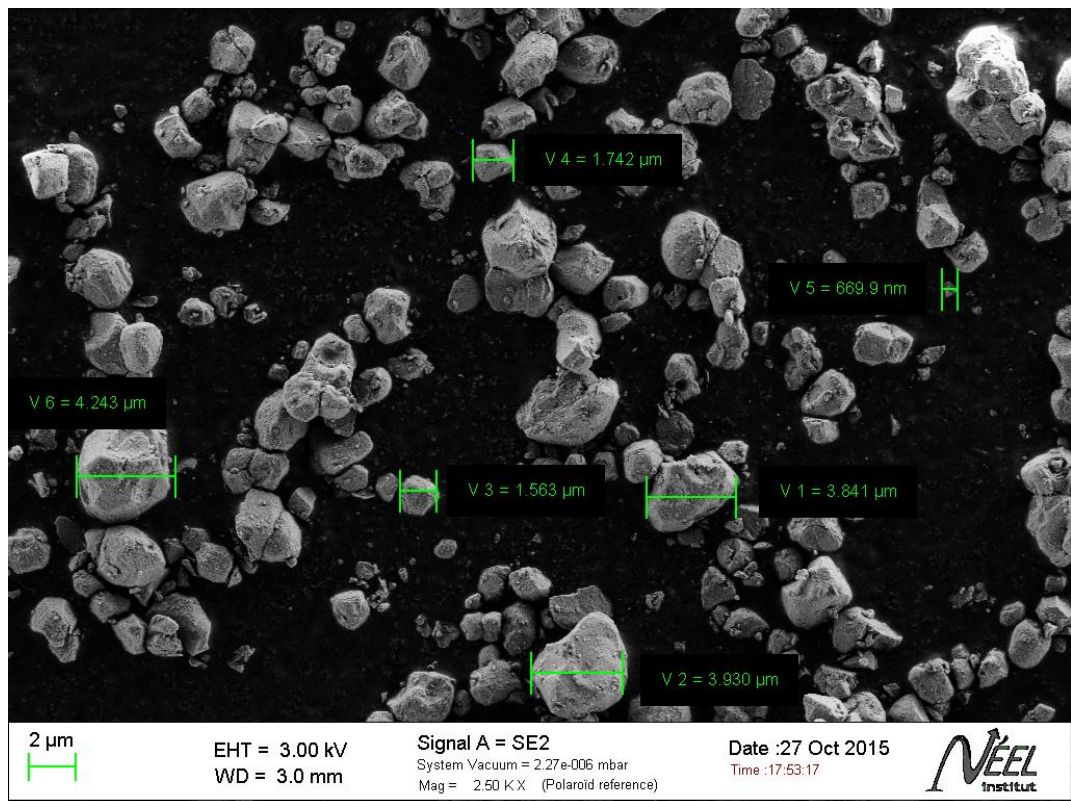


Figure III-1: SEM picture of $\text{Sm}_2\text{Fe}_{17}\text{N}_3$ to give an idea of the size repartition

The Zn powder is produced and supply by the department of nanotechnology of TPU, it has been made by spark erosion technique. The spark erosion technique uses two electrodes of any starting material. Between the two electrodes an electric field is applied and the two electrodes are separated by a small gap. The electric current is higher than the dielectric breakdown field, which produce micro-plasma (sparks). When the spark collapses, vaporized alloy and molten droplets are violently ejected from the boiling regions and propelled through the plasma region into the dielectric liquid where they are very rapidly quenched. This yields the production of nanoparticles used in the reported thermoelectric nanocomposites. For the Zn powder, the wave length of the laser use in the SALD (375nm) is in the band of absorption of Zn, which makes the analysis inefficient. That is why we need to once again use the SEM. The size repartition of our particles is from 1 μm to 10 μm .

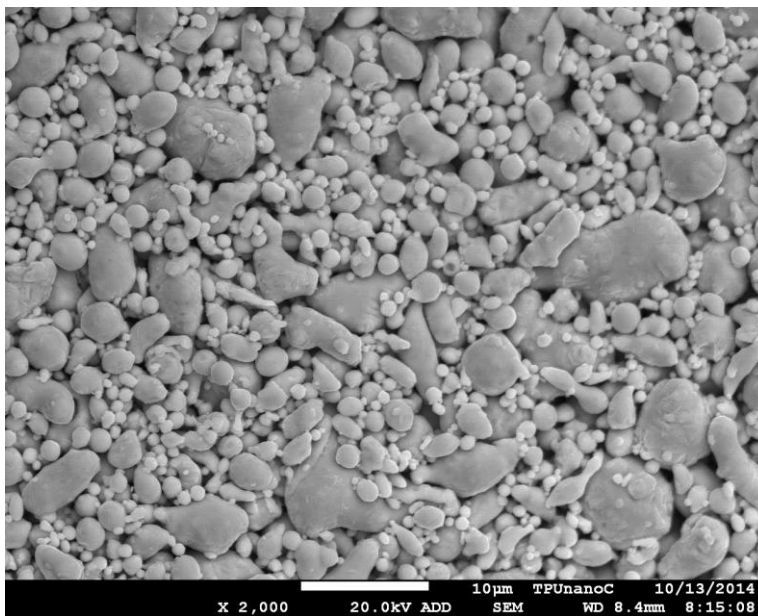


Figure III-2: SEM picture of the Zn powder

To obtain the mix, both powders are dispersed in the hexane (fig. III-4) and put in an ultrasonic bath for 20 min. Then to mix is dry at 60°C to evaporate then hexane, and grinded to break the aggregates made by the drying. The different concentrations made in the laboratory are: 0%, 8%wt, and 15%wt, of Zn. These concentrations have been chosen according to the results in the literature (9) (10).

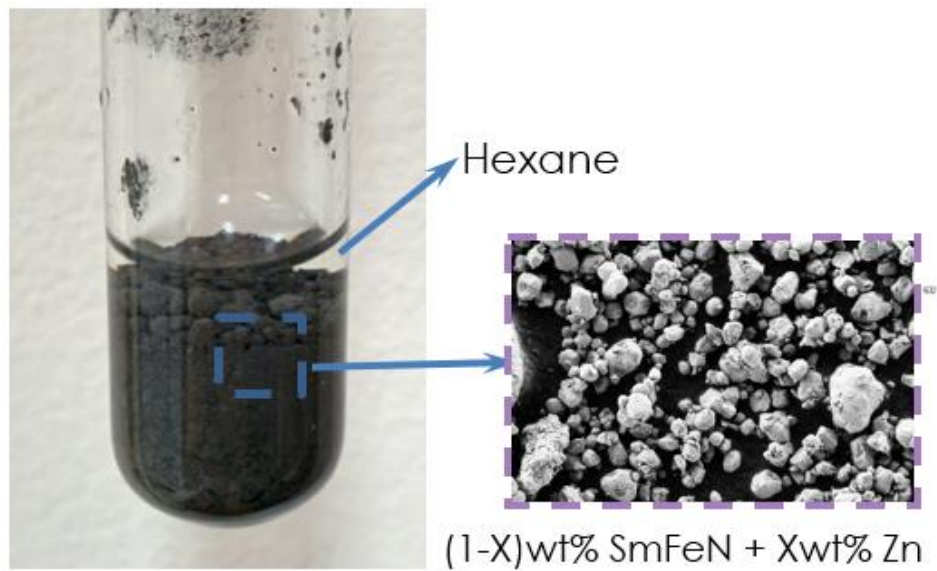


Figure III-4: Picture of Zn + $Sm_2Fe_{17}N_3$ mixture in hexane after ultrasonic bath. (left) SEM picture of the mixture (right).

The XRD analysis of the mixed powder, (figure III-3) shows the presence, of all the components, but also the presence of αFe , before the sintering.

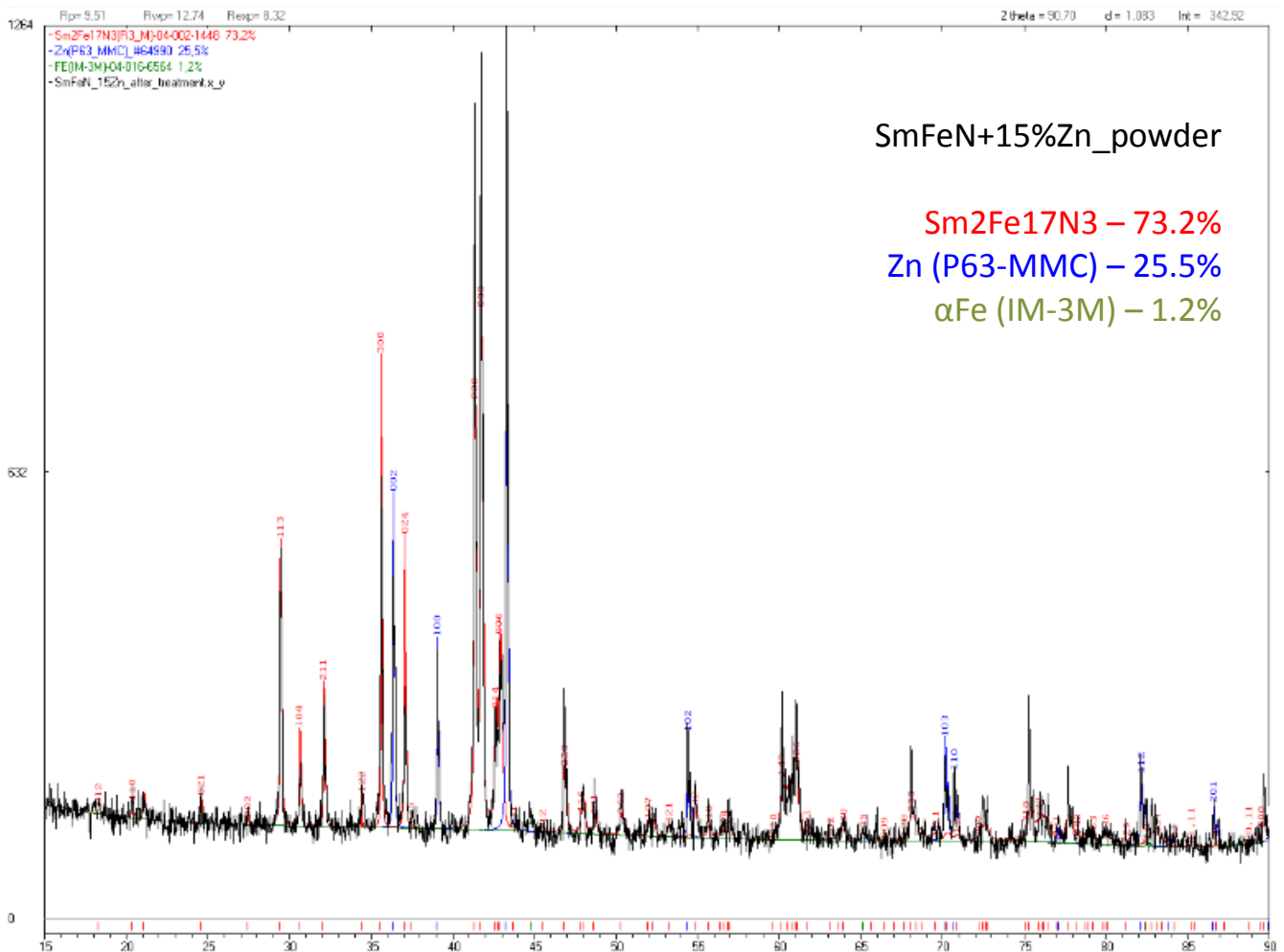


Figure III-3: XRD analysis of 15%Zn+ $Sm_2Fe_{17}N_3$ powder. In red $Sm_2Fe_{17}N_3$, in blue Zn, in green αFe .

B. Magnetic pre-alignment

In order to make the magnetic pre-alignment the powder is put in the tungsten carbide die, and the die is put under an electromagnetic field. This step is done with a custom made device (figure III-5). This step enables alignment of the particles in the good axis before the sintering to obtain the best anisotropy. The effect on the magnetic field on the particles' magnetic moment is described in the figure III-6.

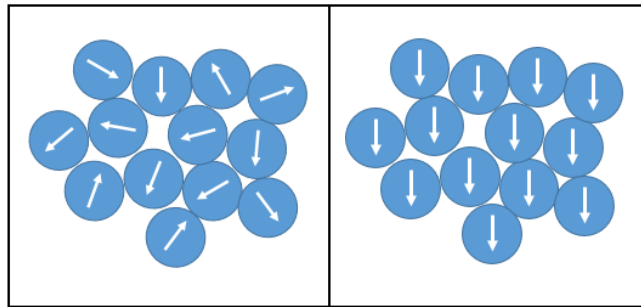


Figure III-6: Representation of the effect of magnetic field on the particles during the pre-alignment. On the left, before alignment, the magnetic moments are randomly oriented. On the right, after pre-alignment, the moment of each particle is aligned in the same direction than the magnetic field.

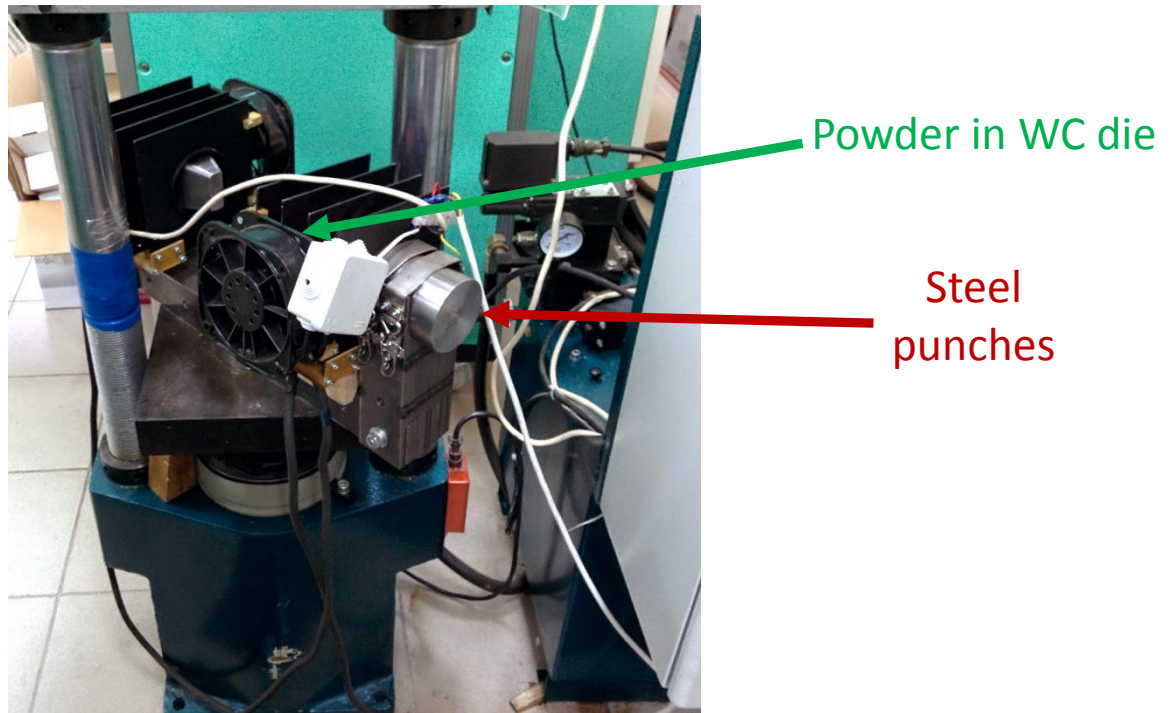


Figure III-5: Picture of the device use to pre-align the powder

C. SPS procedure

The SPS process has been carried out with the supervision of Svetlana PONOMAREVA and Alexei KHASANOV on the DR.SINTER LAB (SPS-515S). The die used is a WC die, we use graphite paper to protect the die from the contamination. The pressure used during the compaction is 155MPa, the time spent the sintering temperature is 5min for all the samples.

The experiments are made with the three different Zn concentrations, at three different temperature, 400°C, 450°C, and 500°C. The name of the samples is indexed in the table III-2.

Tableau III-2: List of the names given to all the sample depending of their concentration of Zn, and sintering temperature.

Content of Zn	Magnetic Pre-alignment	400°C	450°C	500°C
0%wt	0	Sample 0-400n	Sample 0-450n	Sample 0-500n
0%wt	100	Sample 0-400a	Sample 0-450a	Sample 0-500a
8%wt	0	Sample 8-400n	Sample 8-450n	Sample 8-500n
8%wt	100	Sample 8-400a	Sample 8-450a	Sample 8-500a
15%wt	0	Sample15-400n	Sample 15-450n	Sample 15-500n
15%wt	100	Sample15-400a	Sample 15-450a	Sample 15-500a

It has been found than depending of the concentration of Zn the time needed of the process is different. Indeed for main samples the compaction process is ended after 5 min at the sintering temperature, but on the compaction curve on the sample 400-8n (figure III-7) we see that the compaction isn't finished. The compaction time is longer for 8% of Zn than for 15% of Zn.

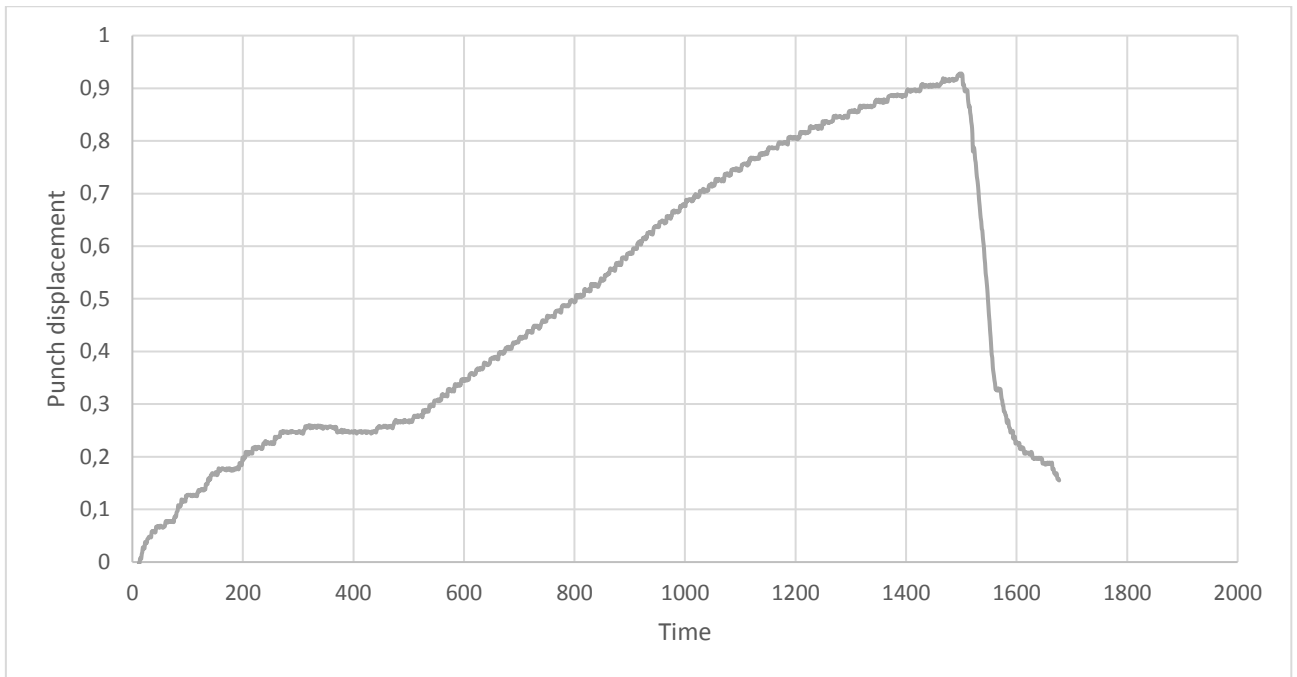


Figure III-7: Compaction curve of the sample 400-8n. In abscise the time is without units. The vertical scale is in cm, it is the displacement of the punch during the compaction

D. Analysis

The magnetic hysteresis loops have been carried out by Svetlana PONOMAREVA in Grenoble, France with the extraction magnetometer.

The XDR analysis has been made under the supervision of Vladimir PAYGIN with the X-Ray diffractometer Shimadzu XRD-7000S with CuK_α target.

The SEM has been made by the professor DVILIS with JSM-7500 FA (JEOL).

**ЗАДАНИЕ ДЛЯ РАЗДЕЛА
«ФИНАНСОВЫЙ МЕНЕДЖМЕНТ, РЕСУРСОЭФФЕКТИВНОСТЬ И
РЕСУРСОСБЕРЕЖЕНИЕ»**

Студенту:

Группа	ФИО
4БМ4И1	ЛУАЗОН ЖОАН ПЬЕР

Институт	физики высоких технологий	Кафедра	наноматериалов и нанотехнологий
Уровень образования	магистратура	Направление подготовки	22.04.01 «Материаловедение и технологии материалов»

Исходные данные к разделу «Финансовый менеджмент, ресурсоэффективность и ресурсосбережение»:

Стоимость ресурсов научного исследования (НИ): материально-технических, энергетических, финансовых, информационных и человеческих	Работа с информацией, представленной в российских и иностранных научных публикациях, аналитических материалах, статистических бюллетенях и изданиях, нормативно-правовых документах.
---	--

Перечень вопросов, подлежащих исследованию, проектированию и разработке:

1. Оценка коммерческого и инновационного потенциала НТИ	Анализ конкурентных технических разработок
2. Планирование процесса управления НТИ: структура и график проведения, бюджет, риски и организация закупок	Иерархическая структура работ План проекта Бюджет проекта
3. Определение ресурсной, финансовой, экономической эффективности	Описание ресурсной эффективности

Перечень графического материала

Table III-1: Raw materials, components and semi-finished products purchased
Table V 2: Price of the device and cost of utilization

Дата выдачи задания для раздела по линейному графику	
--	--

Задание выдал консультант:

Должность	ФИО	Ученая степень, звание	Подпись	Дата
Доцент	Лямина Г.В.	К.х.н., доцент		

Задание принял к исполнению студент:

Группа	ФИО	Подпись	Дата
4БМ4И1	ЛУАЗОН ЖОАН ПЬЕР		

IV. Chapter 5: Financial management

Raw materials, purchased products

Table IV-1: Raw materials, components and semi-finished products purchased

Name	Formula	Quantity (g)	Price per unit (rouble/kg)	Price (rouble)
Samarium Iron Nitride powder	$\text{Sm}_2\text{Fe}_{17}\text{N}_3$	5000	3300	16500
Zinc powder	Zn	500	300	150
total				16650
Comparative product				
Neodymium iron bore powder	$\text{Nd}_2\text{Fe}_{14}\text{B}$	5000	4000	25000
Dysprosium powder	Dy	50	22732,33	1136
Total				26136

According to the table VI-1, for the same weight of powder the Sm-Fe-N is 36% cheaper. This is why it is interesting to elaborate permanent magnets base on Sm-Fe-N.

Table IV-2: Price of the device and cost of utilisation

	Name of equipment	power, kWt	Operating Time (hours per week)	Electricity consumption, rub. per month	Price for the device (\$)
1	Installation for spark plasma sintering «Dr.SINTER LAB 515S»	5	32	720	320 9735
3	Scanning electron microscope JEOL SEM-7500FA	5,5	16	396	150 000
4	diffractometer Shimadzu XRD-7000	5,3	32	763	50 000-100 000
	TOTAL	Over the entire period of the project studies		47842	521 000-571 000